AD-751 588

X-RAY CROSS SECTION COMPILATION FROM 0.1 keV TO 1 MeV

Edith A. Briggs, et al

Kaman Sciences Corporation

Prepared for:

Defense Nuclear Agency

31 August 1972

DISTRIBUTED BY:

NTIS

National Technical Information Service
U. S. DEPARTMENT OF COMMERCE
5285 Port Royal Road, Springfield Va. 22151

AD751588

DNA 2433F
(Formerly DASA 2433)
Supplementary Report
K-72-431(SR)

SUPPLEMENTARY REPORT TO X-RAY CROSS SECTION COMPILATION FROM 0.1 keV TO 1 MeV

DDC
RECEIVED
NOV 22 1972
C

31 August 1972

KAMAN SCIENCES CORPORATION
1500 Garden of the Gods Road
Colorado Springs, Colorado 80907

Reproduced by
NATIONAL TECHNICAL
INFORMATION SERVICE
U S Department of Commerce
Springfield VA 22151

APPROVED FOR PUBLIC RELEASE; DISTRIBUTION UNLIMITED.

ACCESSION for
NTIS
DDC
UNANNOUNCED
JUSTIFICATION
BY
DISTRIBUTION/AVAILABILITY CODES
Dist.
A

DESTROY THIS REPORT WHEN IT IS NO LONGER NEEDED. DO NOT RETURN TO SENDER.

UNCLASSIFIED

Security Classification

DOCUMENT CONTROL DATA - R & D

(Security classification of title, body of abstract and indexing annotation must be entered when the overall report is classified)

1. ORIGINATING ACTIVITY (Corporate author)

Kaman Sciences Corporation
1500 Garden of the Gods Road
Colorado Springs, Colorado 80907

2a. REPORT SECURITY CLASSIFICATION

UNCLASSIFIED

2b. GROUP

3. REPORT TITLE

Supplementary Report to X-Ray Cross Section Compilation from 0.1 keV to 1 MeV.

4. DESCRIPTIVE NOTES (Type of report and inclusive dates)

Final Report Supplement

5. AUTHOR(S) (First name, middle initial, last name)

Edith A. Briggs and Wm. J. Veigele

6. REPORT DATE

31 August 1972

7a. TOTAL NO. OF PAGES

~~75~~ 68

7b. NO. OF REFS

10

8a. CONTRACT OR GRANT NO.

DASA01-70-C-0126

b. PROJECT NO.

NWER: XAXA

c. Task & Subtask: A109

d. Work Unit: 07

9a. ORIGINATOR'S REPORT NUMBER(S)

K-72-431(SR)

9b. OTHER REPORT NO(S) (Any other numbers that may be assigned this report)

DNA 2433F (Formerly DASA 2433)

10. DISTRIBUTION STATEMENT

Approved for public release; distribution unlimited.

11. SUPPLEMENTARY NOTES

12. SPONSORING MILITARY ACTIVITY

Director
Defense Nuclear Agency
Washington, D.C. 20305

13. ABSTRACT

A search of the literature was made for the period from 1920 through June 1972, to obtain experimental x-ray cross sections for the elements in the energy range from 0.1 keV to 1 MeV. Total attenuation and photoelectric absorption data were evaluated and found not to be at variance with values reported in the compilation in the Final Report of this study. New experimental scattering data, along with earlier compiled experimental scattering data, were compared with theoretical values used in the compilation. Data are too scarce and errors are too large to evaluate the theoretical values unequivocally. Low energy theory was explored to determine whether changes in potential, or inclusion of relativistic or correlation effects could significantly improve calculated low energy cross sections. It was concluded that correlation effects would be most important.

DD FORM 1 NOV 65 1473

(a)

UNCLASSIFIED

Security Classification

UNCLASSIFIED
Security Classification

14. KEY WORDS	LINK A ROLE	LINK A WT	LINK B ROLE	LINK B WT	LINK C ROLE	LINK C WT
X-Rays						
Cross Sections						
Attenuation Coefficients						
Attenuation						
Absorption						
Scattering						
Physical Properties						

UNCLASSIFIED
Security Classification

DNA 2433F
(Formerly DASA 2433)
Supplementary Report
K-72-431(SR)

SUPPLEMENTARY REPORT TO X-RAY CROSS SECTION COMPILATION FROM 0.1 keV TO 1 MeV

Kaman Sciences Corporation
Colorado Springs, Colorado 80907

THIS WORK SPONSORED BY THE DEFENSE NUCLEAR AGENCY
UNDER NWER SUBTASK AX109-07

EDITH BRIGGS
and
WM. J. VEIGELE

APPROVED FOR PUBLIC RELEASE; DISTRIBUTION UNLIMITED.

(c)

ABSTRACT

A search of the literature was made for the period from 1920 through June 1972, to obtain experimental x-ray cross sections for the elements in the energy range from 0.1 keV to 1 MeV. Total attenuation and photoelectric absorption data were evaluated and found not to be at variance with values reported in the compilation in the Final Report of this study. New experimental scattering data, along with earlier compiled experimental scattering data, were compared with theoretical values used in the compilation. Data are too scarce and errors are too large to evaluate the theoretical values unequivocally. Low energy theory was explored to determine whether changes in potential or inclusion of relativistic or correlation effects could significantly improve calculated low energy cross sections. It was concluded that correlation effects would be most important.

FOREWORD

This document contains a Supplementary Report to the Final Report, Volumes I and II, DNA 2433F (formerly DASA 2433), Revision 1, KN-71-431(R), which is the final report on contract DASA 01-70-C-0126, amended to cover the period 28 April 1970 - 30 September 1972. This supplemental report is on investigations made at Kaman Sciences Corporation from 6 March 1972 to 30 September 1972 under the direction of Dr. Wm. J. Veigele.

TABLE OF CONTENTS

	Page
ABSTRACT	i
FOREWORD	ii
LIST OF FIGURES	iv
1. INTRODUCTION	1
2. REVIEW OF X-RAY SCATTERING RESEARCH	1
2.1 Coherent Scattering	2
2.1.1 Experimental Values of f	2
2.1.2 Cromer's Form Factors	3
2.1.3 Comparison of Theory with Experimental f Data	4
2.2 Incoherent Scattering	4
2.2.1 Experimental Measurements of Incoherent Scattering	4
2.2.2 Cromer's Incoherent Scattering Functions	5
2.2.3 Comparison of Incoherent Scattering Data	5
2.3 Conclusions from Scattering Study	6
3. TOTAL ATTENUATION	6
4. LOW ENERGY THEORY IMPROVEMENTS	7
4.1 Potential Function	7
4.2 Relativistic Effects	8
4.3 Electron Correlation	9
5. RECOMMENDATIONS	11
5.1 Scattering Cross Sections	11
5.2 Total Attenuation Cross Sections	12
5.3 Low Energy Photoionization Cross Sections	12
REFERENCES	13
APPENDIX: EXPERIMENTAL DATA SOURCES FOR FIGURES	56
DISTRIBUTION LIST	v
DD FORM	xvii

LIST OF FIGURES

		Page
1-20.	Form Factors at Low Momentum Transfer for Be, Ne, Al, Si, Ar, Cr, Fe, Ni, Cu, Ge, Kr, Sn, Xe, Ta, W, Hg, Pb, Bi, Th, and U.	14
21-37.	Form Factors at High Momentum Transfer for Fe, Cu, Zr, Mo, Ag, Cd, In, Sn, I, Ba, Ta, W, Pt, Au, Hg, Pb, and U.	34
38-41.	Incoherent Scattering Functions for Al, Fe, Cu, and Pb.	51
42.	Low Energy Photoionization Cross Sections for Xe.	55

1. INTRODUCTION

This report brings up to date Kaman's research on x-ray attenuation. Recommended sets of cross sections were tabulated and issued in 1971[1]. The present document gives more details concerning certain aspects of x-ray attenuation, particularly developments in the study of x-ray scattering and improvements in low energy theory. Collection of experimental total attenuation cross sections also continued, and data were processed for inclusion in any future compilation or revision.

2. REVIEW OF X-RAY SCATTERING RESEARCH

X-ray scattering and the need for accurate cross sections were explained in Kaman's final report[2] on research in 1967. During that study, a scattering bibliography[3] was also issued. Since then, published accounts of x-ray scattering experiments and papers on related experimental and theoretical work have been obtained and reviewed. Seventeen of the papers reported experimental results on coherent scattering. These results have been added to the graphs from the 1967 compendium on x-ray scattering cross sections. See Figures 1-37. A list of the experimental data sources is in Appendix A. Cromer's[4] recent form factor calculations appear on the graphs with other theoretical curves and extend the range of theory for comparison with experiment. Cromer's calculated values for both form factors and incoherent scattering functions were compared with experimental data.

A need continues for more accurate bound electron cross sections over a continuous range of energy. Though there are many theories for calculating scattering cross sections, few experiments have been conducted that help evaluate the reliability of the theoretical cross sections, especially for incoherent scattering. The present work pertains to x-ray scattering from electrons bound in normal atoms of a material.

2.1 Coherent Scattering

Coherent scattering is that which results in a change in x-ray momentum but no change in energy and, therefore, no deposition of energy in the scattering material. The coherent scattering cross section is the probability of occurrence of such an interaction under given conditions.

At very low energy the contribution of x-ray scattering is negligible when compared with photoelectric absorption as the most likely attenuating event. In hydrogen, the occurrence of coherent scattering begins to affect total attenuation, though only slightly, at about 1 keV. Coherent scattering cross sections decrease with increase in energy, but their influence as a significant proportion of attenuation increases because photoelectric absorption cross sections decrease more rapidly as energy increases to 10 - 100 keV. Depending upon atomic number, the frequency of coherent and incoherent scattering is about equal at 10 - 100 keV.

2.1.1 Experimental Values of f

Experimental data for coherent scattering were reduced to form factors f and plotted as f/Z versus sin $(\theta/2)/\lambda$ (Å)

for comparison. Recent experimental data seem to agree with earlier data.

New experimental data are for beryllium, and tungsten at low energy. The data agree with other results. Iron and nickel data from data source 1 (see Figs. 7 and 8) are lower than other experimental data between sin $(\theta/2)/\lambda$ of 0.2 and 0.5.

Uncertainties are high, probably higher than the reported errors, because error bars do not overlap in many cases. In general, the graphs that include more recent experimental measurements of x-ray scattering are as incomplete and inconsistent as before, and as difficult to interpret with the accuracy desired.

2.1.2 Cromer's Form Factors

Cromer[4] recently computed form factors for all elements over a broader energy range than previously covered by theoretical calculations. Cromer's data, which were compiled in Ref. 1, were plotted on the graphs containing experimental and other theoretical coherent scattering cross sections shown in Figs. 1-37.

Cromer's coherent scattering factors agree closely with Hartree-Fock data from earlier sources to sin $(\theta/2)/\lambda \cong 3$, where the old HF data ended. Atomic structure is noticeable in the graphs of Cromer's data, as it is in the earlier HF calculations. Beyond $\sin(\theta/2)/\lambda = 10$, the curves of f/Z are somewhat subjective because the calculated f values do not follow a smooth curve and intervals between values are

greater. Curves representing the Thomas-Fermi theory turn out sharply at about $\sin(\theta/2)/\lambda = 10$ and end uncertainly. Thus we have no theoretical comparison farther out on the graphs except that of Cromer.

2.1.3 Comparison of Theory with Experimental f Data

Below $\sin(\theta/2)/\lambda \cong 3$ there is good agreement between Comer's[4] values and experimental data except for Si, Ni, Pb, Bi, Th, and U. For those elements, however, the experiments contained large uncertainties.

Above $\sin(\theta/2)/\lambda \cong 3$ form factors are calculated at such wide intervals they cannot be plotted without uncertainty and comparison with experimental data in this region is more difficult.

2.2 Incoherent Scattering

Incoherent scattering from electrons is scattering that results in a change in both momentum and energy of the incident photon and a deposition of energy in the scattering material. The incoherent scattering cross section gives the probability of occurrence of this interaction with electrons in matter. Incoherent scattering starts to influence total attenuation cross sections near 1 keV. The importance of incoherent scattering grows until it predominates in the total attenuation process at higher energies (10 keV for Z = 2, 600 keV for Z = 94).

2.2.1 Experimental Measurements of Incoherent Scattering

From Ref. 2, the experimental incoherent scattering functions that could be compared with theory were those

from entire atoms rather than from individual electron shells. These data were replotted versus the variable $\sin(\theta/2)/\lambda$ (Å) in Figs. 38 - 41. The range of experimental data for aluminum and copper extends only to $\sin(\theta/2)/\lambda = 2$. Experimental values for iron go to $\sin(\theta/2)/\lambda = 35$, and to 50 for lead. Still this coverage is very scanty for drawing general conclusions.

2.2.2 Cromer's Incoherent Scattering Functions

To evaluate Cromer's[4] incoherent scattering function calculations, data in Volume II of Reference 1 were divided by atomic number and plotted as S on the graphs of experimental data in Figs. 38 - 41.

2.2.3 Comparison of Incoherent Scattering Data

Whole atom experimental data for incoherent scattering were compared with Cromer's[4] theoretical incoherent scattering factors. For comparison with theoretical calculations, incoherent scattering data were plotted versus $\sin(\theta/2)/\lambda$ (Å), although that unit is not an exact momentum transfer variable for incoherent scattering. (See Reference 2).

Experimental data for the four elements agree qualitatively with theoretical curves. Disagreement between theory and experiment appears greatest at low $\sin(\theta/2)/\lambda$ (Å), where error bars in general do not touch the theoretical curve. There also is general disagreement for back scattering where theory predicts $S \leq 1$ but some experiments show $S > 1$. Data source 31 is the only paper with data for more than one element. The values there are above the theoretical curves.

The experimental errors are so large and so few data are available that no accurate quantitative conclusions can be drawn.

2.3 Conclusions from Scattering Study

In conclusion, Cromer's[4] form factor values, which provide the most comprehensive set available, agree quite well with experimental data over the regions examined. For high values of sin $(\theta/2)/\lambda$, his calculations are not comprehensive enough to be plotted smoothly to obtain good quantitative comparisons.

Cromer's values for incoherent scattering functions agree qualitatively with experimental data, but because of the scarcity of and large errors on incoherent experimental data, unequivocal quantitative comparisons are impossible. Cromer's theory, like earlier ones, also predicts $S \leq 1$ at large angles but many experiments and recent theories indicate that $S > 1$ in the back scattering region.

It is recommended that Cromer's values continue to be used in the cross section compilation, until further calculations and experiments have been made.

3. TOTAL ATTENUATION

Measurements of total attenuation have been reported since our compilation of x-ray cross sections[1] was distributed. A survey of the values from the recently obtained published papers with comparable data shows no present need for revising attenuation cross-section values. Additional ranges

covered by the recent experimental data are mainly between 0.1 keV and 1 keV for chromium, nickel, zirconium, and molybdenum, and from 0.2 keV to 1.74 keV for germanium.

4. LOW ENERGY THEORY IMPROVEMENTS

Consideration was given to improving low energy photoionization cross section calculations by investigating the effects of three phenomena -- the potential function, relativity, and electron correlations.

4.1 Potential Function

Photoionization cross sections are calculated in the dipole approximation from the equation[5]

$$\tau_{n\ell} = \frac{4\pi\alpha\, a_o^2}{3} N_{n\ell}\, h\nu \left[\left(\frac{\ell}{2\ell+1}\right) R^2_{\ell-1} + \left(\frac{\ell+1}{2\ell+1}\right) R^2_{\ell+1}\right] \qquad (1)$$

where α is the fine structure constant, a_o is the Bohr radius, $N_{n\ell}$ is the subshell occupation number, and $R_{\ell\pm1}$ are radial matrix elements for bound and continuum states. The radial matrix elements are given by

$$R_{\ell\pm1} = \int_0^\infty P_{n\ell}(r)\, r\, P_{\varepsilon,\ell\pm1}(r)\, dr \qquad (2)$$

where ε is the continuum electron energy, and $P_{n\ell}(r)$ and $P_{\varepsilon,\ell\pm1}(r)$ are bound and continuum radial wave functions obtained by solving the Schrödinger equation in atomic units,

$$\left[\frac{d^2}{dr^2} + V(r) + E_n - \frac{\ell(\ell+1)}{r^2}\right]P(r) = 0. \qquad (3)$$

Here E_n is total energy of an n shell electron and V(r) is the central potential.

A self consistent field solution of Eq. (3) yields P(r) values which are used in Eq. (2) to get the $R_{\ell\pm1}$ which are used in Eq. (1). For the bound state these $P_{n\ell}(r)$ have consistent values of V(r) which together give a minimum energy. This, in general, will differ from the experimental value. It was considered that a parametric variation of V(r) could be attempted to give a final set of E_n equal to experimental values. These would produce a set of $P'_{n\ell}$ (r) different from those obtained if no restriction were imposed on the E_n. These $P'_{n\ell}$ (r) then would give more accurate values of τ.

This method was tested for selected elements and energies by introducing experimental E_n and varying V(r) and $P_{n\ell}(r)$ iteratively until their changes were small. The resulting $P_{n\ell}(r)$ were used in Eq. (2), and Eq. (1) was used to calculate $\tau_{n\ell}$.

Differences of less than a few percent in $\tau_{n\ell}$ calculated by both methods for selected elements and energies, imply that a parametric variation in the potential function would not significantly improve low energy photoionization cross sections.

4.2 Relativistic Effects

Most of the discrepancy between our low energy theory and experiment results from the use of the approximate Slater

exchange potential and not from relativistic effects. There are comparable (and competing) corrections to the outer shell binding energies of Xe resulting from the inclusion of relativity and complete exchange, but the exchange effect is more significant than the relativistic effect for calculation of photoelectric cross sections. For example, Figure 42 from Kennedy and Manson[6] shows recent HF (complete exchange) calculation for the photoelectric cross section of Xe between 100 and 1000 eV and our HFS values[1]. The discrepancy below about 200 eV can only be due to our incomplete exchange, since both calculations are nonrelativistic and the Kennedy and Manson calculation seems to match experiment rather well.

In any single-particle model, electrons that are photoelectrically excited by photons in the 0.1 to 1 keV range are not relativistic for any element. The Slater exchange approximation seems to be fairly good for cross section calculations down to about 100 eV and is very good at energies greater than about 200 or 300 eV where outer shell effects are less significant.

4.3 Electron Correlation

A review of the literature was made to determine the expected importance of electron correlations, to evaluate recent developments in correlation effects in photoionization theory, and to see whether comparisons of theories with experiments show the effects of correlations.

It is known and has been stated explicitly by Slater[7] that it is the lack of correlation in the Hartree-Fock method

that keeps it from being exact. He also concludes that exact wave functions are important in calculating photoionization cross sections because the matrix elements are very sensitive to small errors in wave functions because of their oscillatory behavior.

It was stated also by Larsson and Calais[8] that correlation effects may be comparatively strong for valence electrons in regions of low electron density. Generally, this includes the low energy region from 0.1 keV to 10 keV.

Correlation is introduced into atomic wave functions by using not only single electron wave functions $\psi(r_i)$, or their products, but also functions of the form $\psi(r_{ij})$ where the i and j refer to different electrons. Wave functions containing as many as 220 terms[9] for low Z atoms have been developed, but generating wave functions of this type for larger atoms is very difficult. Other wave functions are available but many have not been tried in photoionization calculations. Even models for generating them have not been studied extensively. The homogeneous electron gas model expressions for correlation potentials are known[8] to good approximation. These may be best for valence electrons and should be considered for improving low energy calculations.

Other methods of including correlation include a generalized form[10] of Eq. (3)

$$\left[\frac{d^2}{dr^2} + V(r) + E - \frac{\ell'(\ell'+1)}{r^2} - (2/r)\sum_{ik} A_{ik}\, Y^i_k\, (P_i, P_i)\right] P^{(1)}_{E\ell'}(r) =$$

$$(2/r)\sum_{ik} B_{ik}\, Y^i_k\, (P_i, P^{(1)}_{E\ell'})P_i(r) + \sum_i{}' \lambda_i\, P_i(r) \qquad (4)$$

where the correlation effects are included in the numerical coefficients A_{ik} and B_{ik}. This approach can be considered for improving low energy theory by introducing correlation effects directly in the Schrodinger equation.

There have been few reliable experiments, over only restricted energy regions, and mostly on low Z elements, against which to compare theory. The state of theory should be evaluated further and approximate methods of introducing correlations should be examined or developed.

5. RECOMMENDATIONS

After a review of experimental data, a comparison of scattering theory with experiments, and an investigation of the possibilities of improving photoionization theory, the following recommendations are given. Their implementation would improve the quality of x-ray cross sections for normal atoms to the degree required by DNA users for the present and immediate future.

5.1 Scattering Cross Sections

Because of the scarcity of and large uncertainties in experimental incoherent scattering data, and the wide variations in theoretical and experimental data, additional experiments are recommended. These should be on the entire atom as well as on particular electron shells and should be done at all angles, especially in the back-scatter region.

To assist in evaluating theory, it is recommended that Cromer's incoherent scattering functions be calculated for

individual electron shells, at least for those elements for which there are experimental data for individual shells.

Additional coherent scattering experiments are recommended in all energy regions and scattering angles for all elements. Cromer's form factors should be calculated at smaller intervals above $\sin(\theta/2)/\lambda = 10$ to reduce theoretical uncertainty and improve comparison with experimental results.

5.2 Total Attenuation Cross Sections

To replace interpolated and extrapolated cross sections with values substantiated by experiment, attenuation measurements are needed for elements and energies that have no data, or sparse or inconsistent data.

5.3 Low Energy Photoionization Cross Sections

The region of greatest uncertainty in photon cross sections is below 10 keV because there are relatively few accurate experimental data to verify theoretical calculations. Measurements in this region for all elements and for individual electron shells are recommended.

The theory used at Kaman and described in Reference 1 can be modified, as discussed in Section 4, to calculate low energy cross sections with the accuracy required by DNA. A program for this is strongly recommended.

REFERENCES

1. Veigele, Wm. J., E. Briggs, L. Bates, E. M. Henry and B. Bracewell, "X-Ray Cross Section Compilation from 0.1 keV to 1 MeV", DNA 2433F, Kaman Sciences Corp., Colorado Springs, Colo., 31 July 1971.

2. Veigele, Wm. J., "Research on X-Ray Scattering Cross Sections", KN-738-67-3(R), Kaman Nuclear, Colorado Springs, Colo., 31 August 1967.

3. Veigele, Wm. J., "X-Ray Scattering Bibliography", KN-738-67-2(R), Kaman Nuclear, Colorado Springs, Colo., 30 June 1967.

4. Cromer, D. T., personal communcation and J. Chem. Phys. 50, 4857 (1969). D. T. Cromer and J. B. Mann, J. Chem. Phys. 47, 1892 (1967); A24, 321 (1968). D. T. Cromer and J. T. Waber, Acta Cryst. 18, 104 (1965).

5. Bethe, H. A. and E. E. Salpeter, Quantum Mechanics of One- and Two-Electron Atoms (Springer-Verlag, Berlin, 1957) 295.

6. Kennedy, D. J. and S. T. Manson, Phys. Rev. A 5, 227 (1972).

7. Slater, J. C., Quantum Theory of Atomic Structure, Vol. II (McGraw-Hill Book Co., Inc., New York, 1960) 32.

8. Larsson, S. and J. L. Calais, Chem. Phys. Letters 14, 12 (1972).

9. Crossley, R. J. S. in: D. R. Bates and I. Estermann, ed., Advances in Atomic and Molecular Physics, Vol. V (Academic Press, New York, 1969), 237.

10. Fano, U. and J. W. Cooper, Rev. Mod. Phys. 40, 441 (1968).

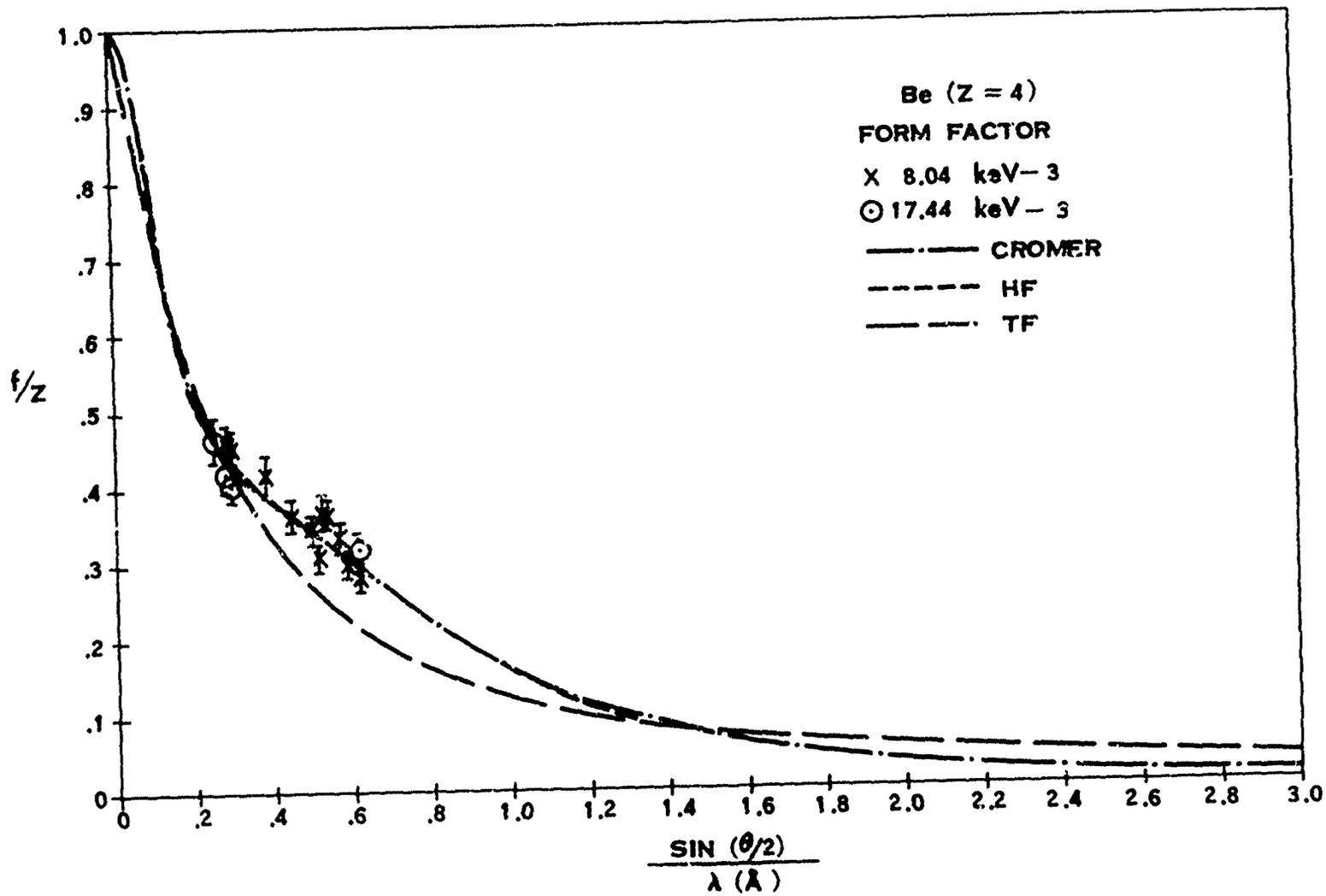
Be (Z = 4)
FORM FACTOR
X 8.04 keV – 3
⊙ 17.44 keV – 3
CROMER
HF
TF
f/Z
1.0
.9
.8
.7
.6
.5
.4
.3
.2
.1
0
0
.2
.4
.6
.8
1.0
1.2
1.4
1.6
1.8
2.0
2.2
2.4
2.6
2.8
3.0
SIN (θ/2) / λ (Å)

FIGURE 1

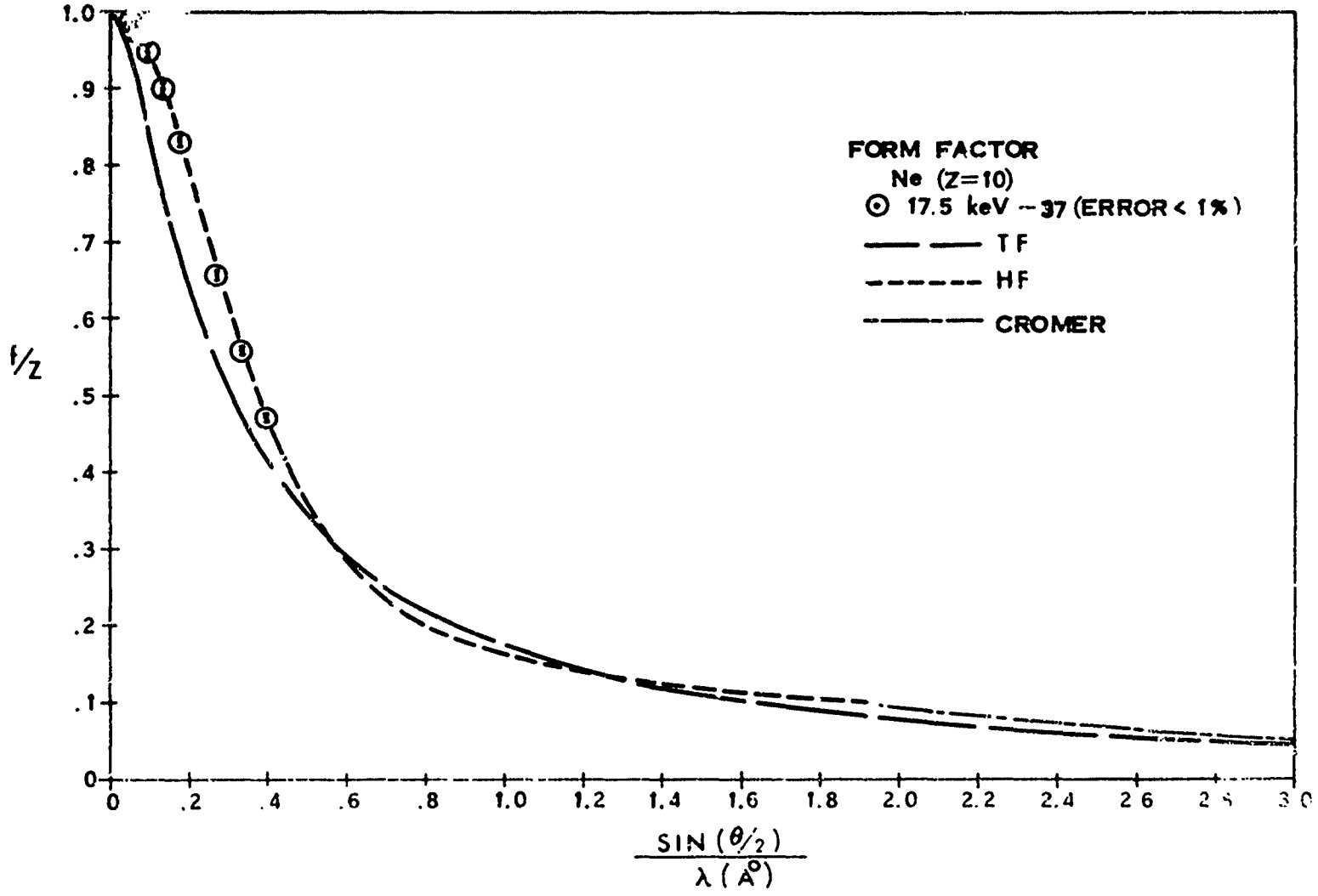
FORM FACTOR
Ne (Z=10)
17.5 keV – 37 (ERROR < 1%)
TF
HF
CROMER
f/Z
1.0
.9
.8
.7
.6
.5
.4
.3
.2
.1
0
0
.2
.4
.6
.8
1.0
1.2
1.4
1.6
1.8
2.0
2.2
2.4
2.6
3.0
SIN (θ/2)
λ (Å)

FIGURE 2

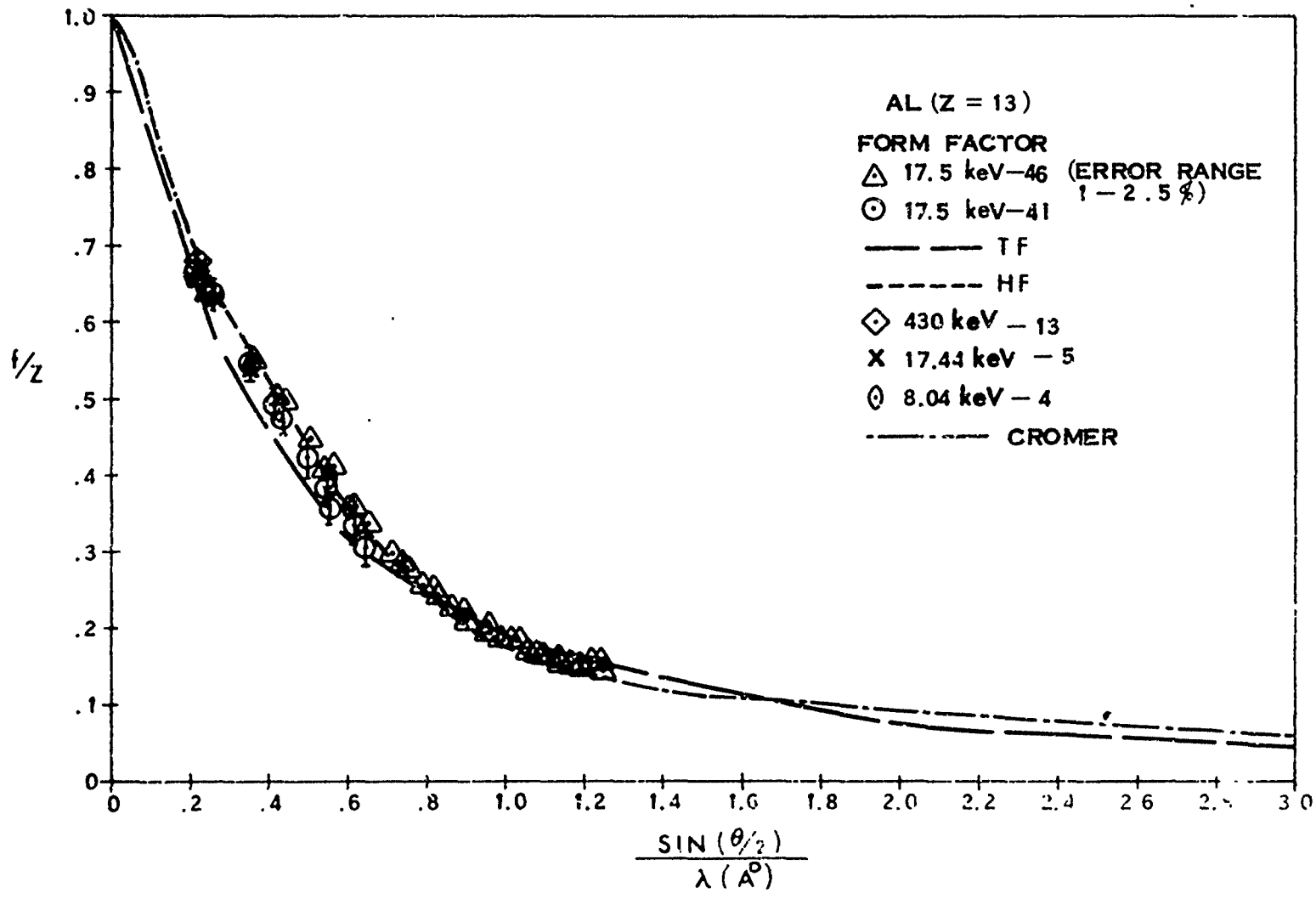
AL (Z = 13)
FORM FACTOR
17.5 keV—46 (ERROR RANGE 1 — 2.5 %)
17.5 keV—41
TF
HF
430 keV — 13
X 17.44 keV — 5
8.04 keV — 4
CROMER
f/Z
1.0
.9
.8
.7
.6
.5
.4
.3
.2
.1
0
0
.2
.4
.6
.8
1.0
1.2
1.4
1.6
1.8
2.0
2.2
2.4
2.6
3.0
SIN (θ/2) / λ (A°)

FIGURE 3

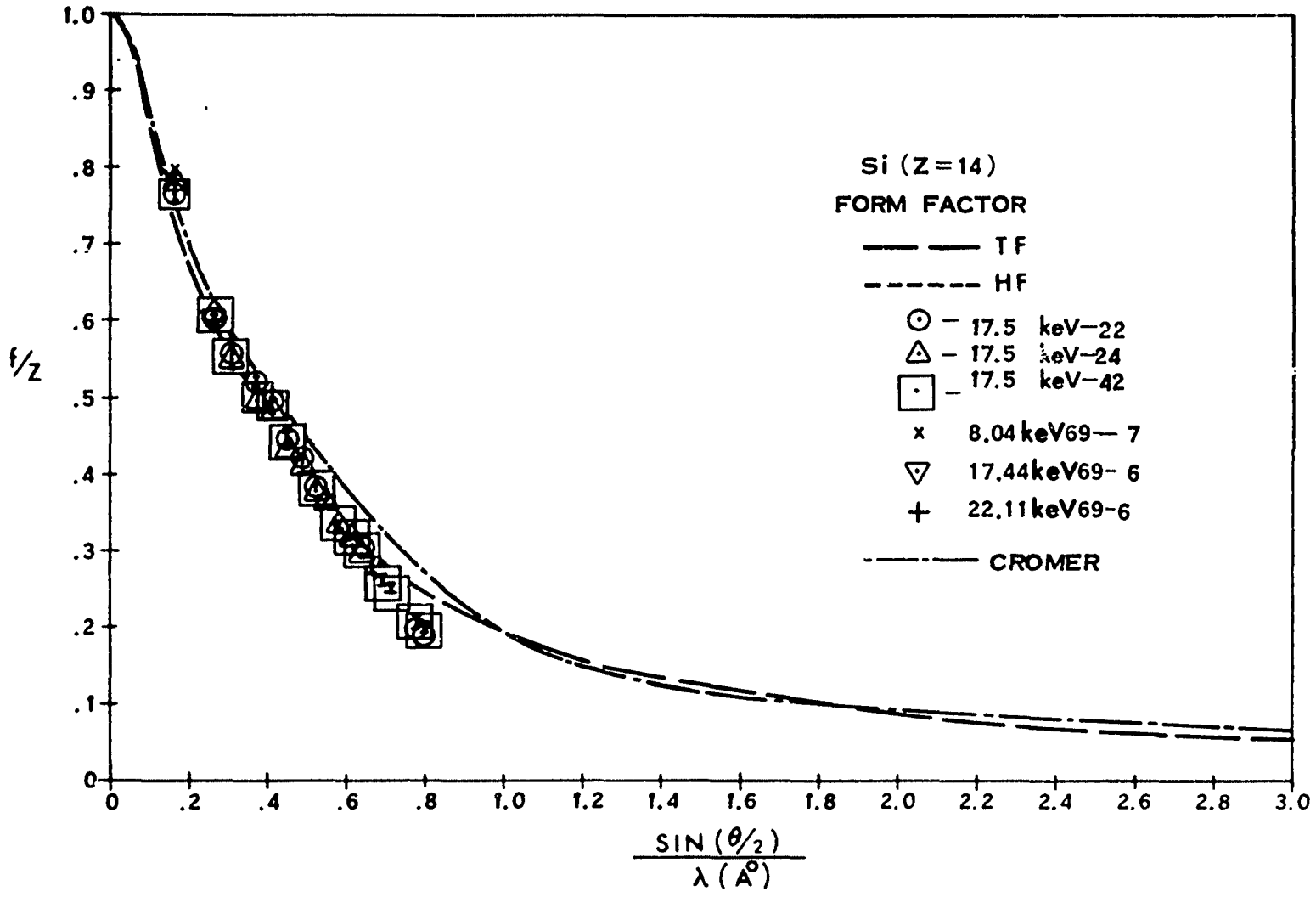
Si (Z=14)
FORM FACTOR
TF
HF
17.5 keV—22
17.5 keV—24
17.5 keV—42
8.04 keV69— 7
17.44 keV69- 6
22.11 keV69-6
CROMER
f/Z
SIN (θ/2) / λ (Å)
1.0
.9
.8
.7
.6
.5
.4
.3
.2
.1
0
0
.2
.4
.6
.8
1.0
1.2
1.4
1.6
1.8
2.0
2.2
2.4
2.6
2.8
3.0

FIGURE 4

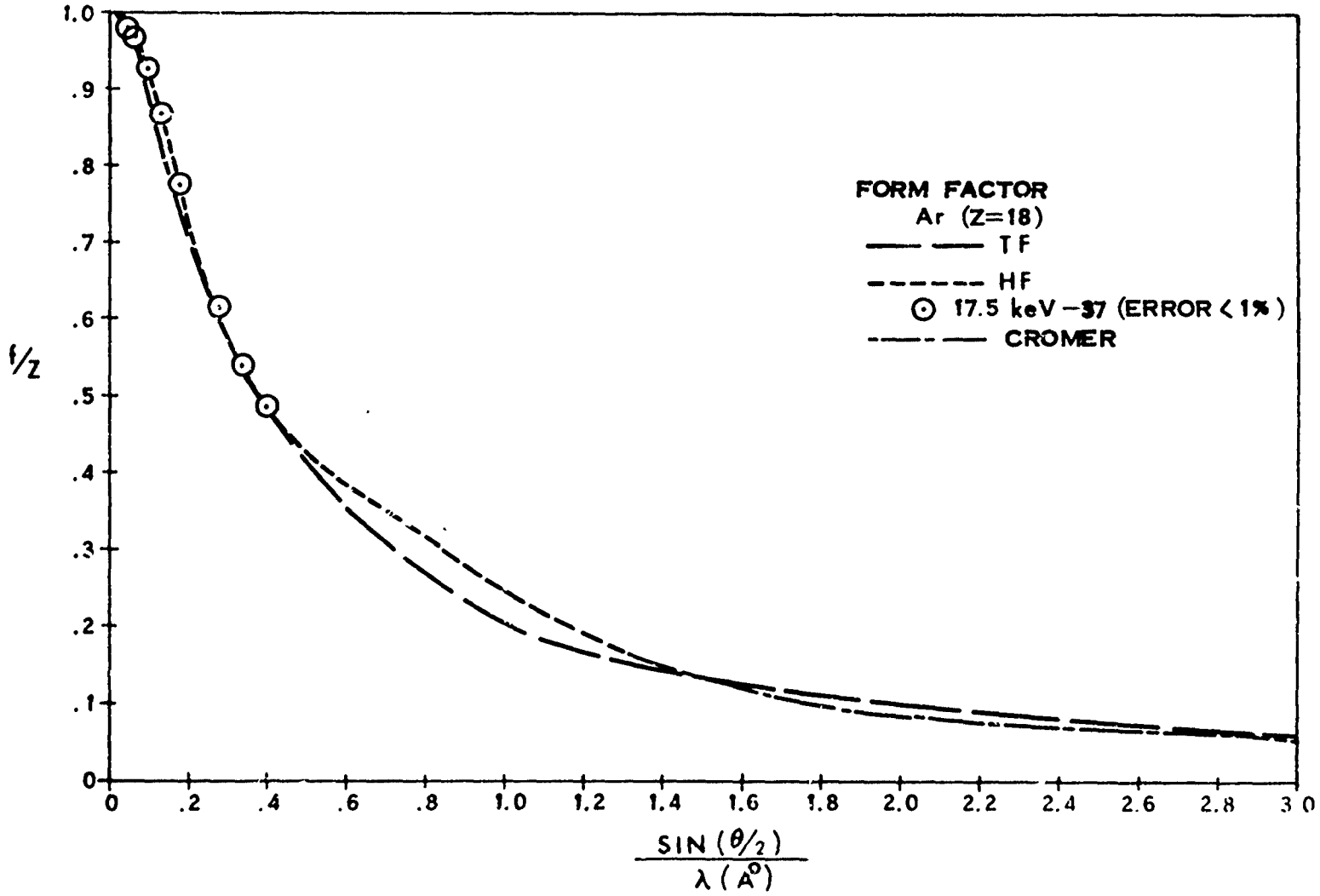
FORM FACTOR
Ar (Z=18)
TF
HF
17.5 keV –37 (ERROR < 1%)
CROMER
f/Z
1.0
.9
.8
.7
.6
.5
.4
.3
.2
.1
0
0
.2
.4
.6
.8
1.0
1.2
1.4
1.6
1.8
2.0
2.2
2.4
2.6
2.8
3.0
SIN (θ/2) / λ (A°)

FIGURE 5

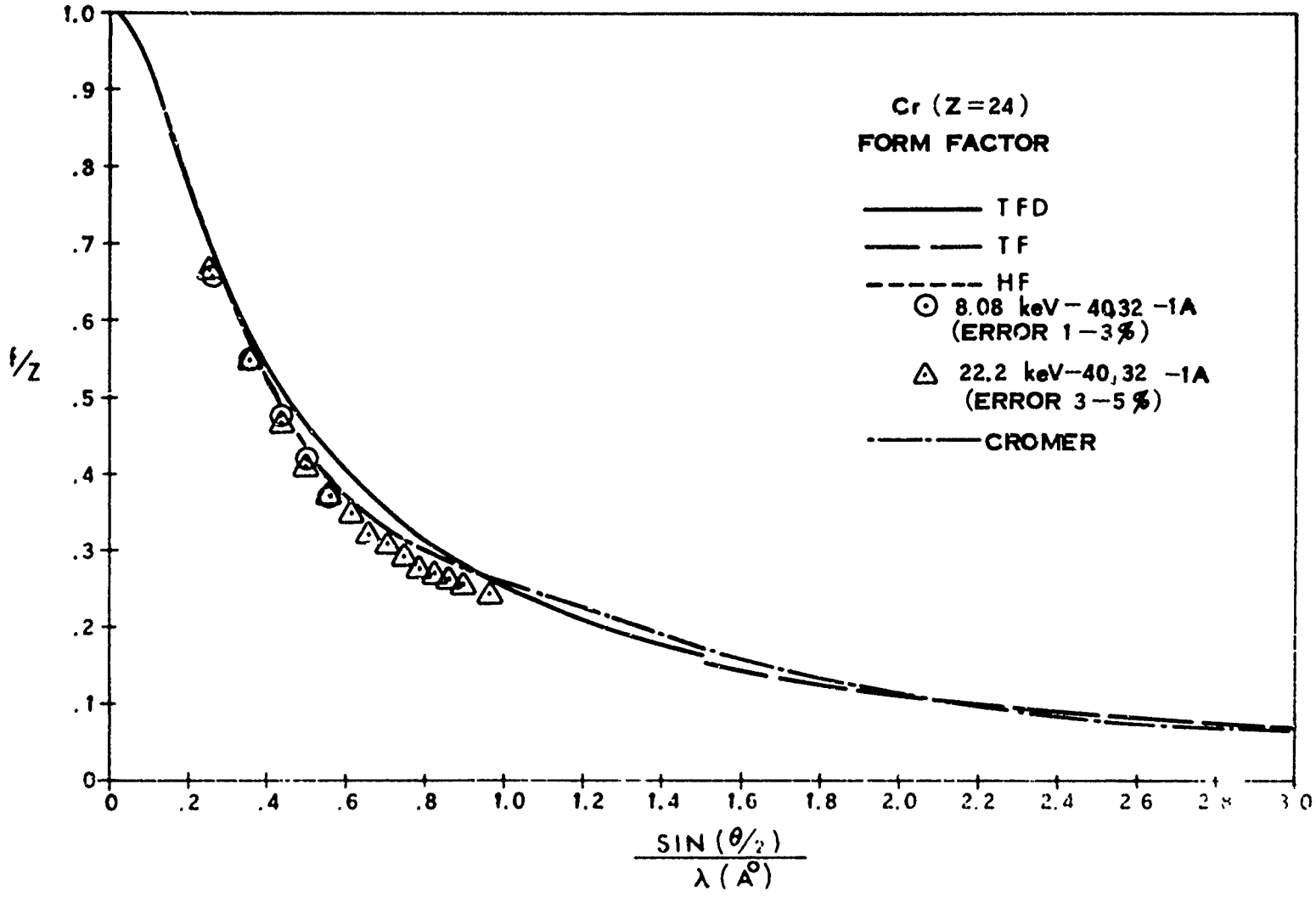
Cr (Z=24)
FORM FACTOR
TFD
TF
HF
8.08 keV – 40,32 –1A
(ERROR 1–3%)
22.2 keV–40,32 –1A
(ERROR 3–5%)
CROMER
f/Z
1.0
.9
.8
.7
.6
.5
.4
.3
.2
.1
0
0
.2
.4
.6
.8
1.0
1.2
1.4
1.6
1.8
2.0
2.2
2.4
2.6
2.8
3.0
SIN (θ/2)
λ (A°)

FIGURE 6

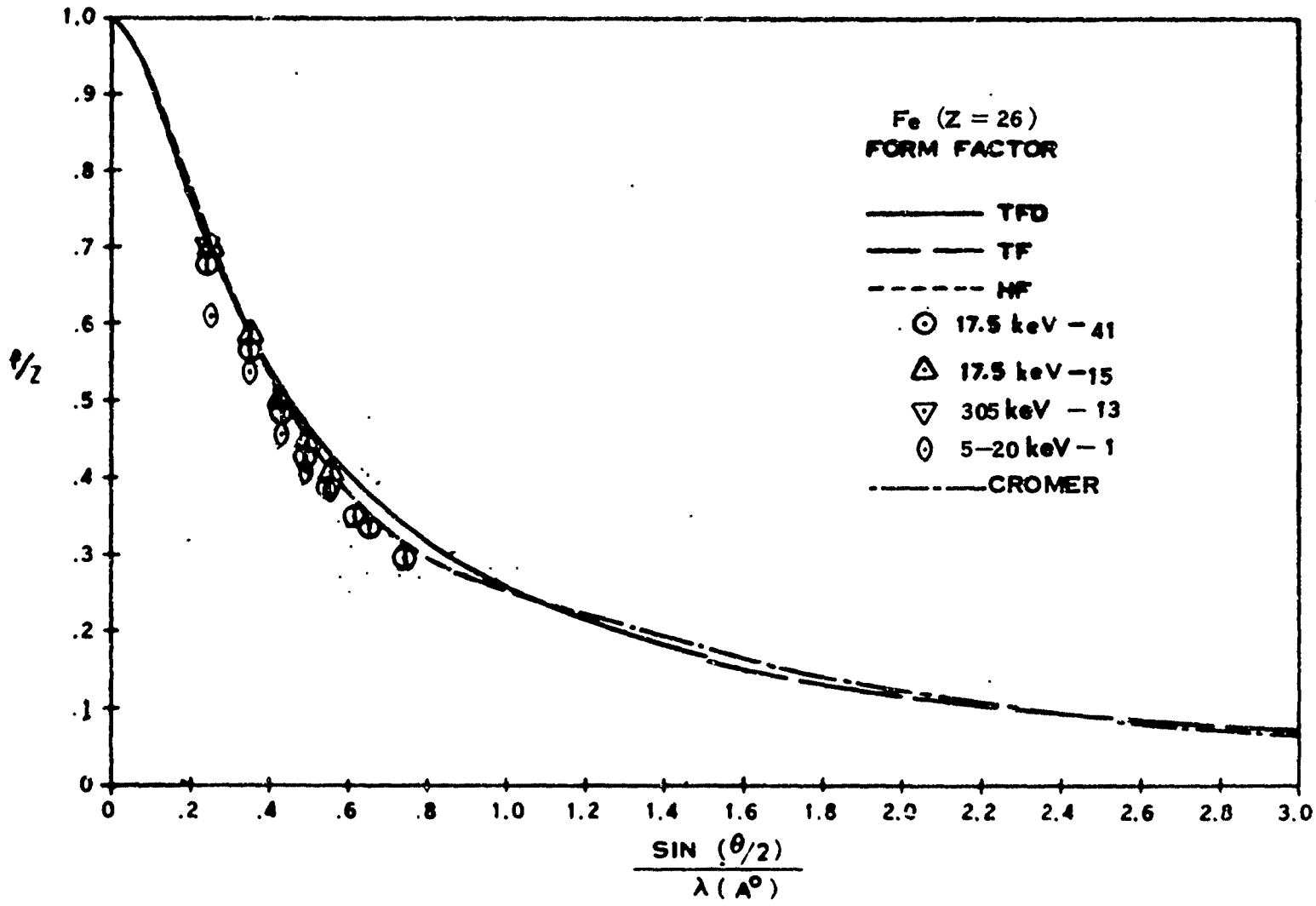
Fe (Z = 26)
FORM FACTOR
TFD
TF
HF
17.5 keV – 41
17.5 keV – 15
305 keV – 13
5–20 keV – 1
CROMER
f/Z
1.0
.9
.8
.7
.6
.5
.4
.3
.2
.1
0
0
.2
.4
.6
.8
1.0
1.2
1.4
1.6
1.8
2.0
2.2
2.4
2.6
2.8
3.0
SIN (θ/2) / λ (A°)

FIGURE 7

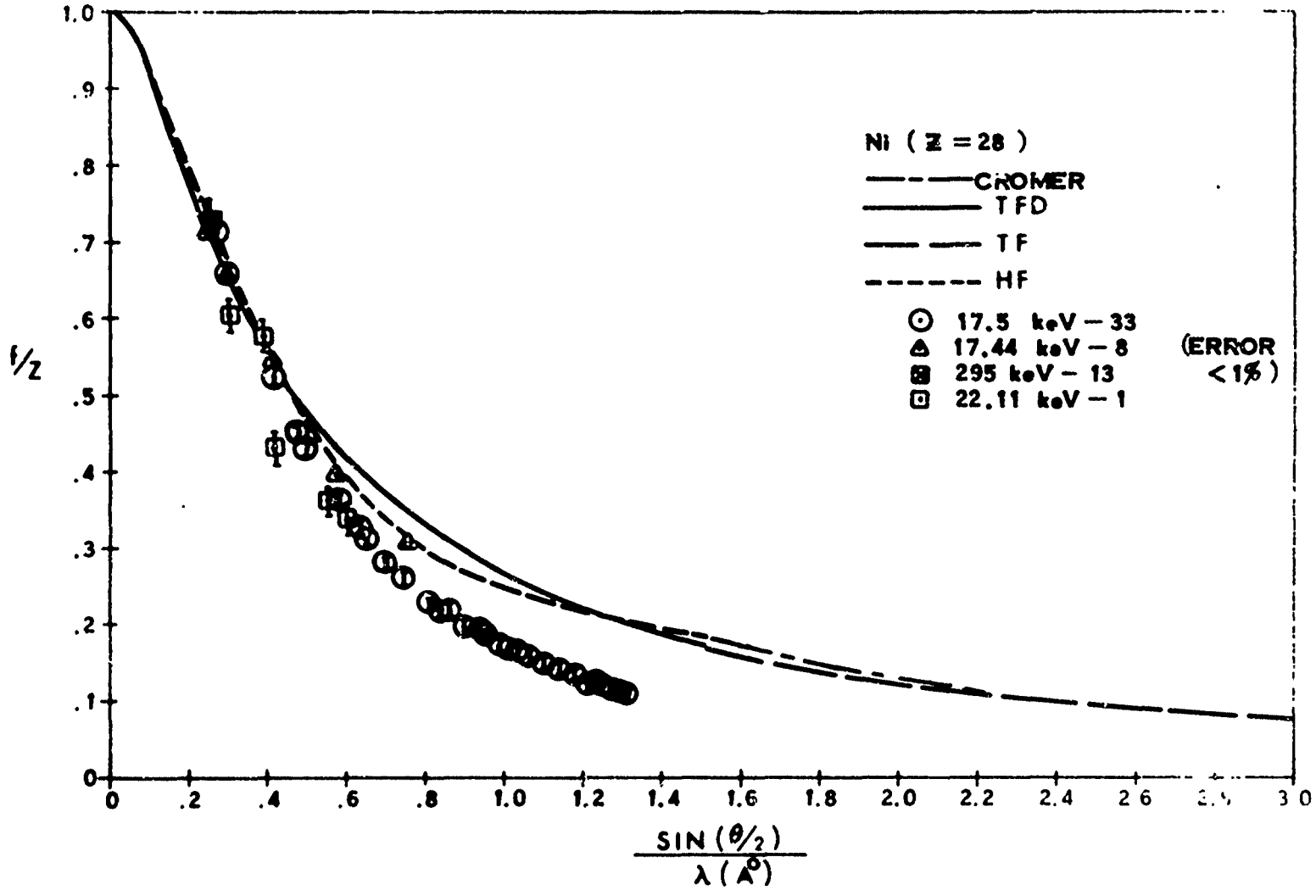
Ni (Z = 28)
CROMER
TFD
TF
HF
17.5 keV — 33
17.44 keV — 8
295 keV — 13
22.11 keV — 1
(ERROR < 1%)
f/Z
SIN (θ/2) / λ (Å)
1.0
.9
.8
.7
.6
.5
.4
.3
.2
.1
0
.2
.4
.6
.8
1.0
1.2
1.4
1.6
1.8
2.0
2.2
2.4
2.6
3.0

FIGURE 8

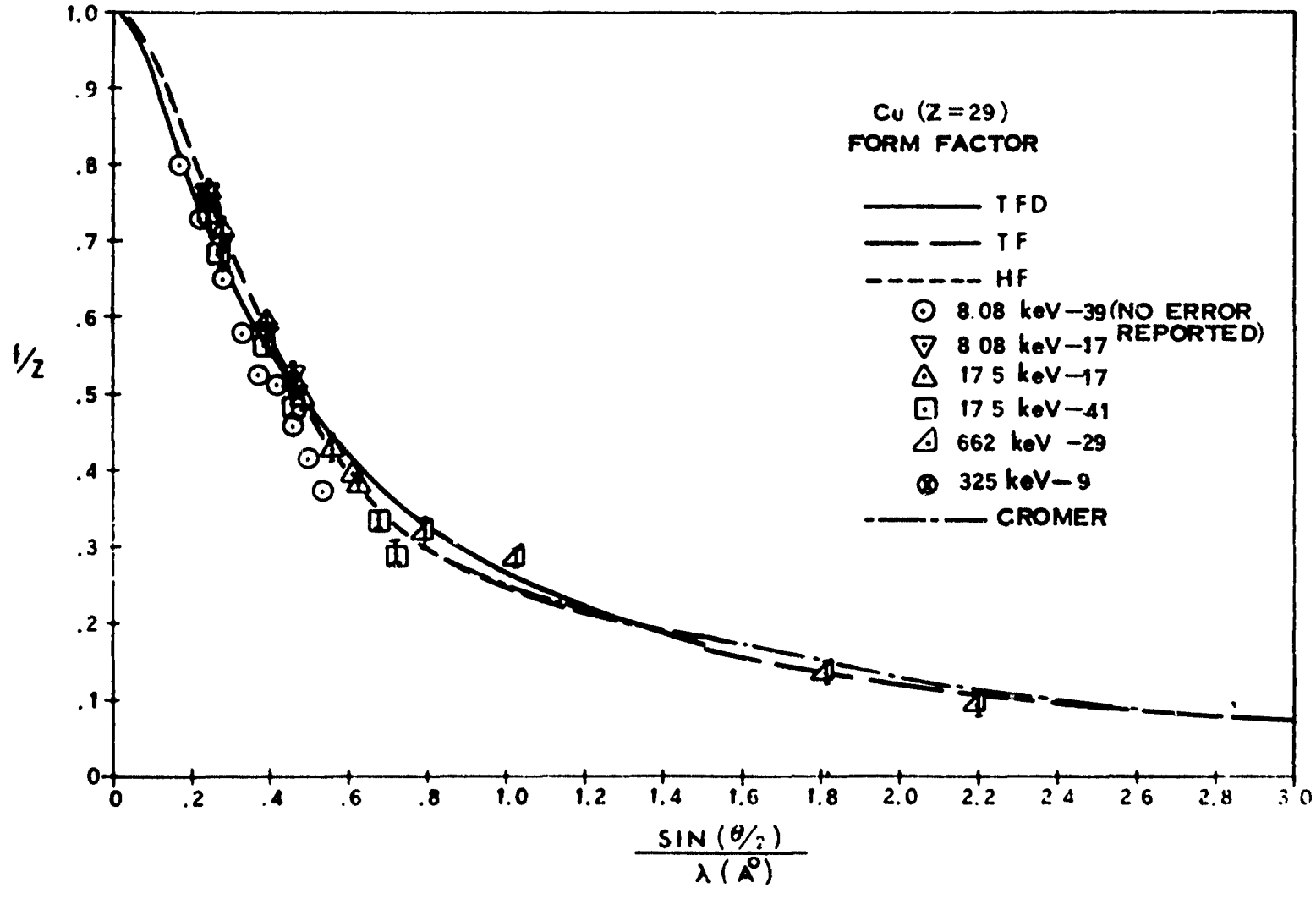
Cu (Z=29)
FORM FACTOR
TFD
TF
HF
8.08 keV—39 (NO ERROR REPORTED)
8 08 keV—17
17 5 keV—17
17 5 keV—41
662 keV —29
325 keV—9
CROMER
f/Z
1.0
.9
.8
.7
.6
.5
.4
.3
.2
.1
0
0
.2
.4
.6
.8
1.0
1.2
1.4
1.6
1.8
2.0
2.2
2 4
2 6
2.8
3 0
SIN (θ/2)
λ (Å)

FIGURE 2

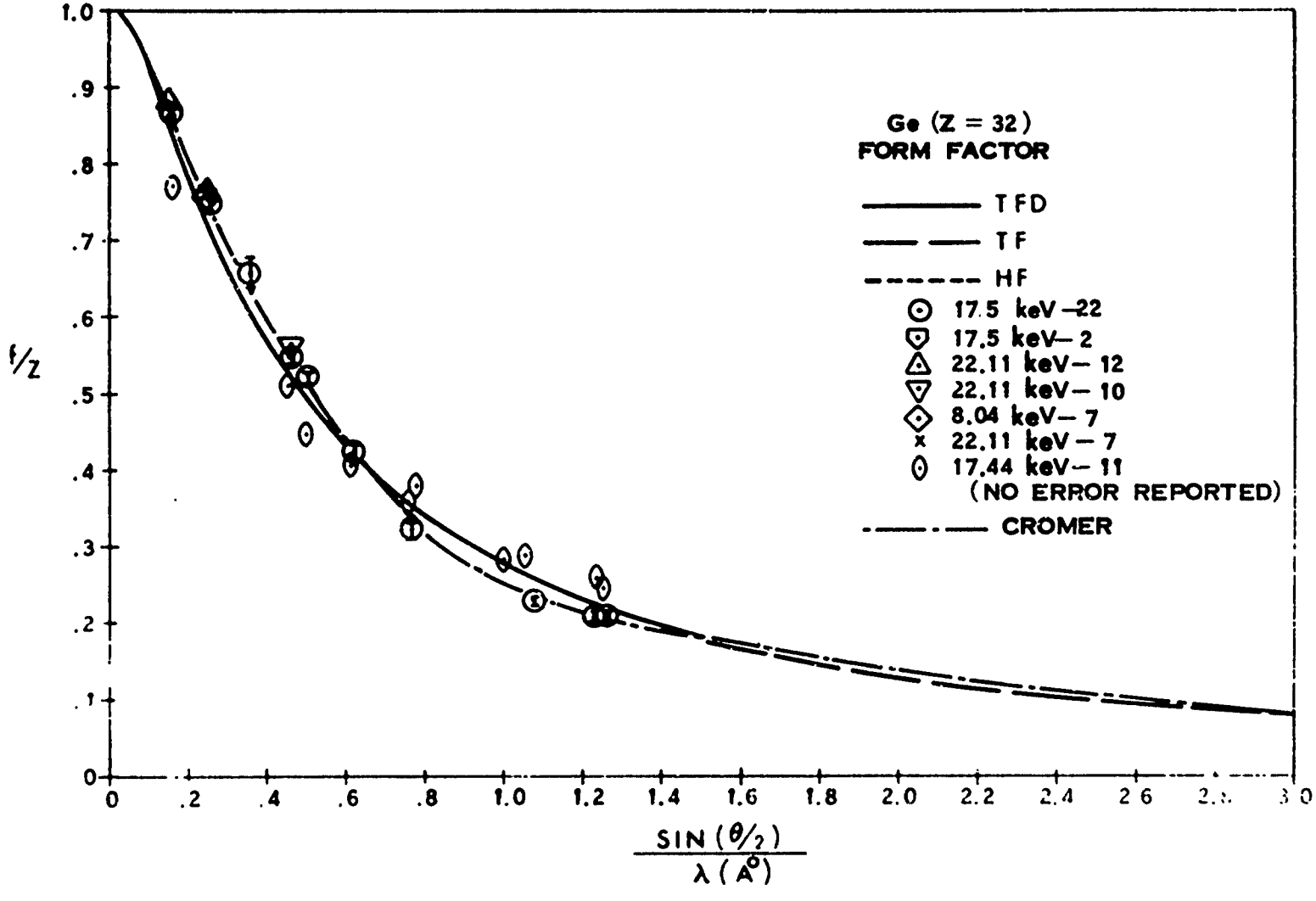
Ge (Z = 32)
FORM FACTOR
TFD
TF
HF
17.5 keV–22
17.5 keV– 2
22.11 keV– 12
22.11 keV– 10
8.04 keV– 7
22.11 keV – 7
17.44 keV– 11
(NO ERROR REPORTED)
CROMER
f/Z
1.0
.9
.8
.7
.6
.5
.4
.3
.2
.1
0
0
.2
.4
.6
.8
1.0
1.2
1.4
1.6
1.8
2.0
2.2
2.4
2.6
3.0
SIN (θ/2)
λ (A°)

FIGURE 10

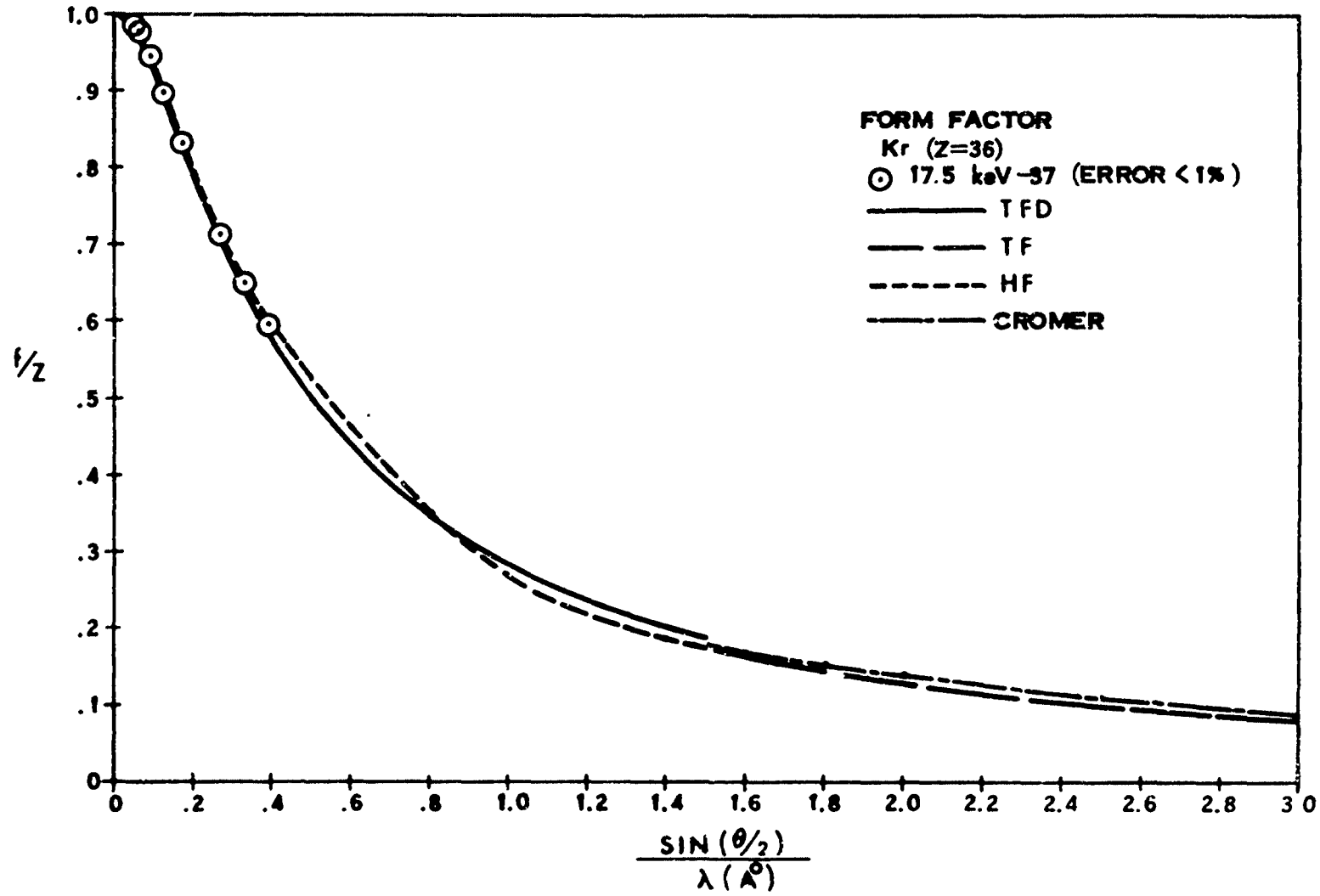
FORM FACTOR
Kr (Z=36)
17.5 keV-37 (ERROR < 1%)
TFD
TF
HF
CROMER
f/Z
1.0
.9
.8
.7
.6
.5
.4
.3
.2
.1
0
0
.2
.4
.6
.8
1.0
1.2
1.4
1.6
1.8
2.0
2.2
2.4
2.6
2.8
3.0
SIN (θ/2) / λ (Å)

FIGURE 11

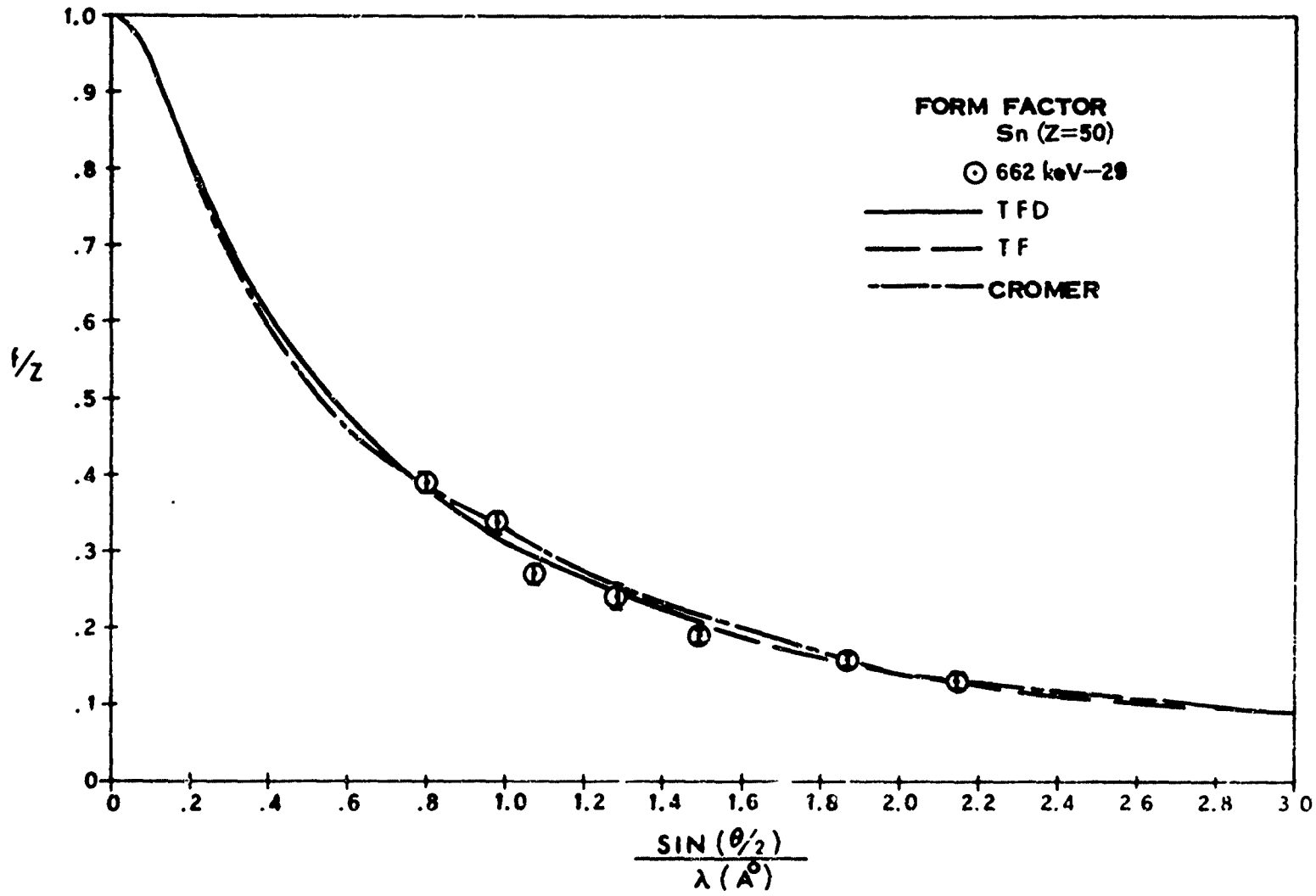
FORM FACTOR
Sn (Z=50)
662 keV—29
TFD
TF
CROMER
f/Z
1.0
.9
.8
.7
.6
.5
.4
.3
.2
.1
0
0
.2
.4
.6
.8
1.0
1.2
1.4
1.6
1.8
2.0
2.2
2.4
2.6
2.8
3.0
SIN (θ/2) / λ (Å)

FIGURE 12

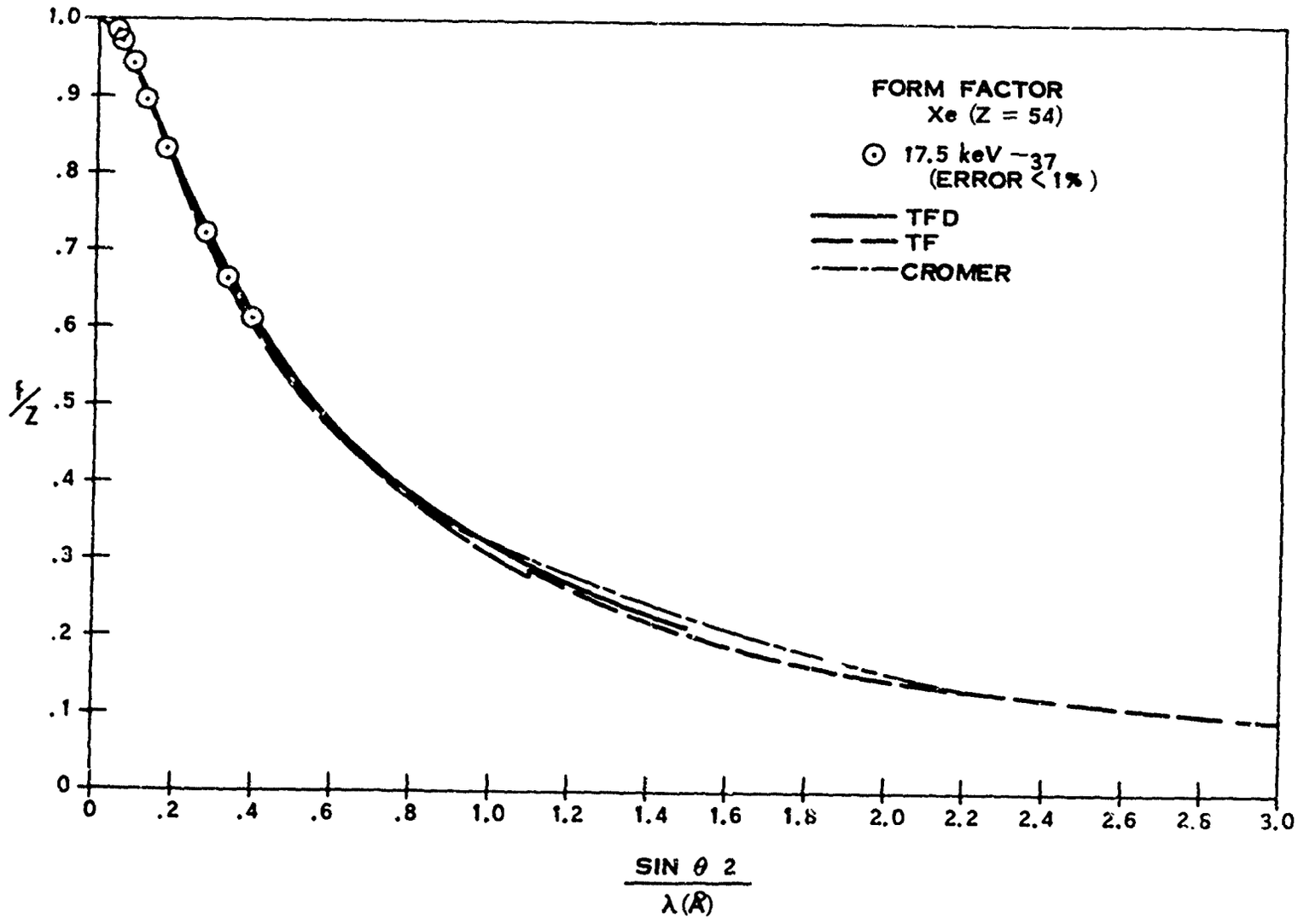
FORM FACTOR
Xe (Z = 54)
17.5 keV
(ERROR < 1%)
TFD
TF
CROMER
f/Z
1.0
.9
.8
.7
.6
.5
.4
.3
.2
.1
0
0
.2
.4
.6
.8
1.0
1.2
1.4
1.6
1.8
2.0
2.2
2.4
2.6
2.8
3.0
SIN θ 2 / λ (Å)

FIGURE 13

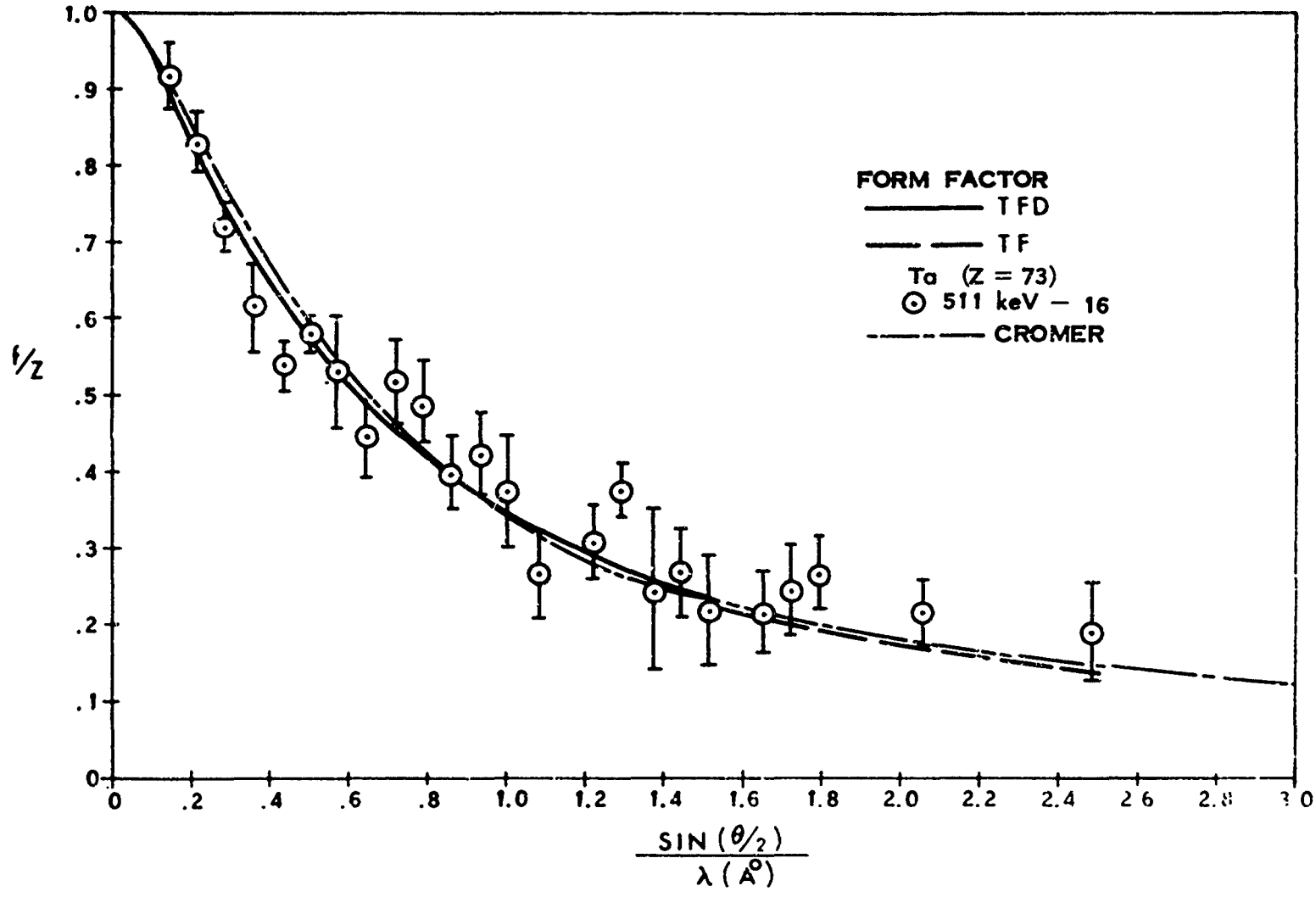
FORM FACTOR
TFD
TF
Ta (Z = 73)
511 keV – 16
CROMER
f/Z
1.0
.9
.8
.7
.6
.5
.4
.3
.2
.1
0
0
.2
.4
.6
.8
1.0
1.2
1.4
1.6
1.8
2.0
2.2
2.4
2.6
2.8
3.0
SIN (θ/2) / λ (A°)

FIGURE 14

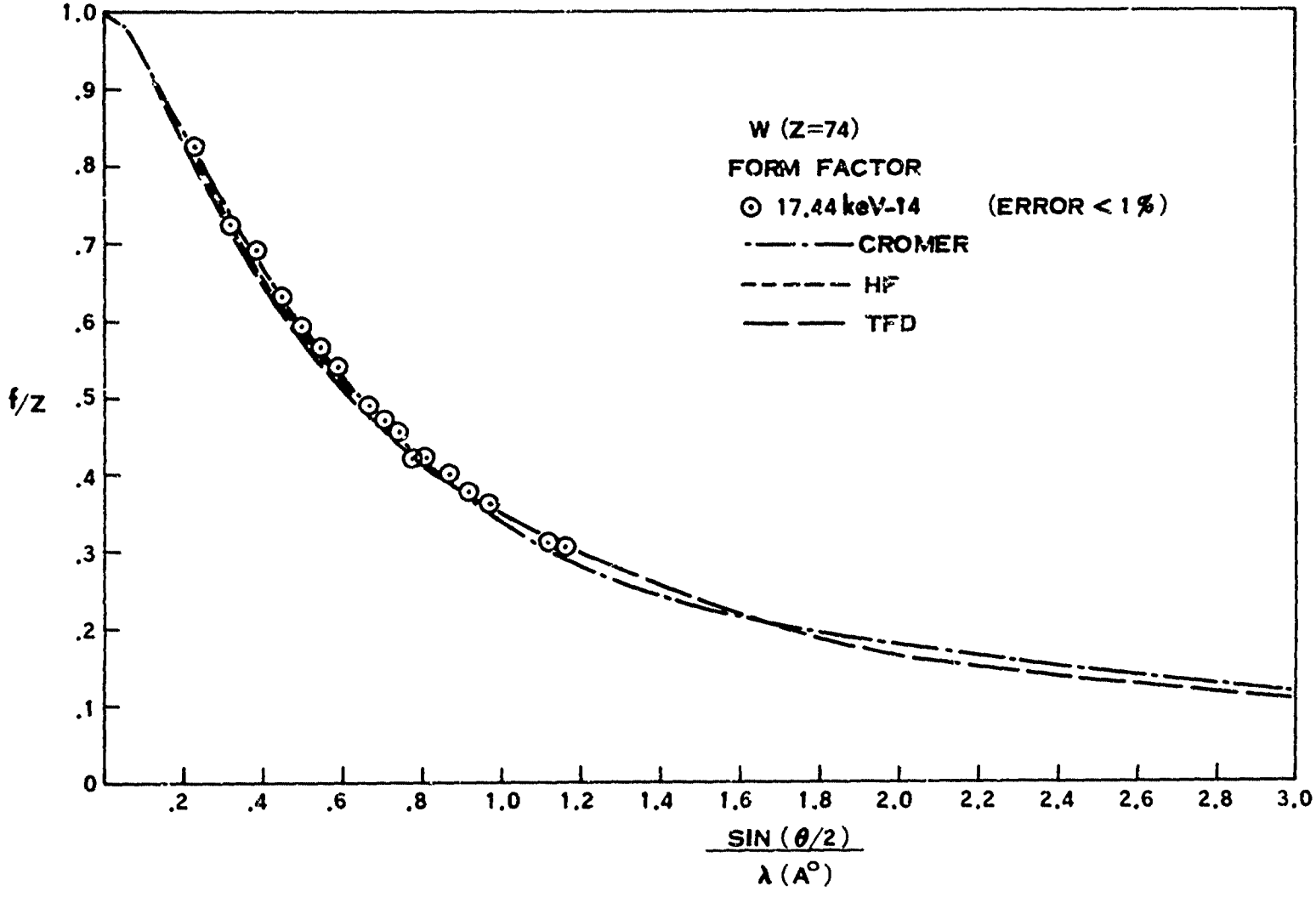
W (Z=74)
FORM FACTOR
⊙ 17.44 keV-14 (ERROR < 1 %)
CROMER
HF
TFD
f/Z
1.0
.9
.8
.7
.6
.5
.4
.3
.2
.1
0
.2
.4
.6
.8
1.0
1.2
1.4
1.6
1.8
2.0
2.2
2.4
2.6
2.8
3.0
SIN (θ/2) / λ (A°)

FIGURE 15

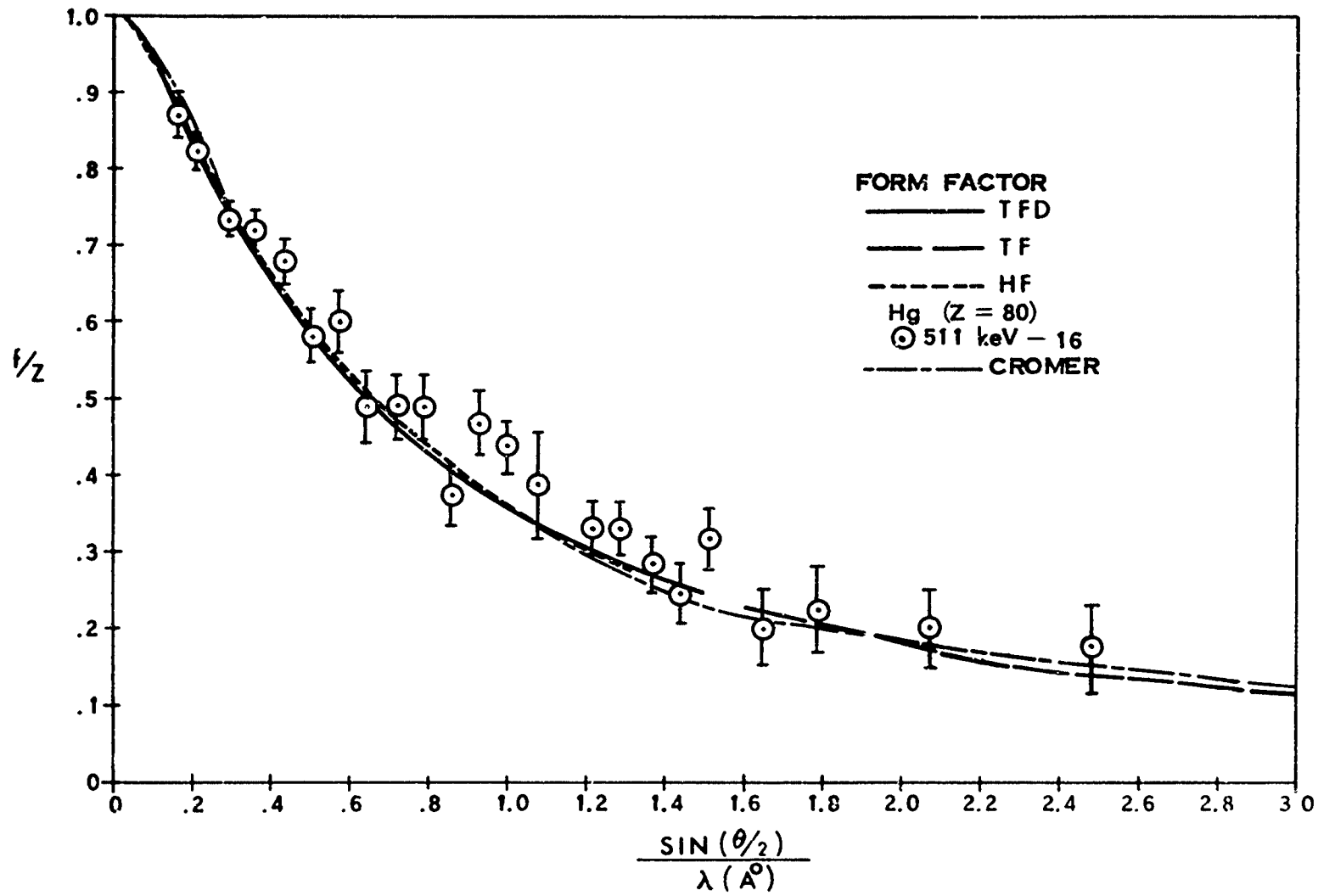
FORM FACTOR
TFD
TF
HF
Hg (Z = 80)
511 keV – 16
CROMER
f/Z
1.0
.9
.8
.7
.6
.5
.4
.3
.2
.1
0
0
.2
.4
.6
.8
1.0
1.2
1.4
1.6
1.8
2.0
2.2
2.4
2.6
2.8
3.0
SIN (θ/2) / λ (Å)

FIGURE 16

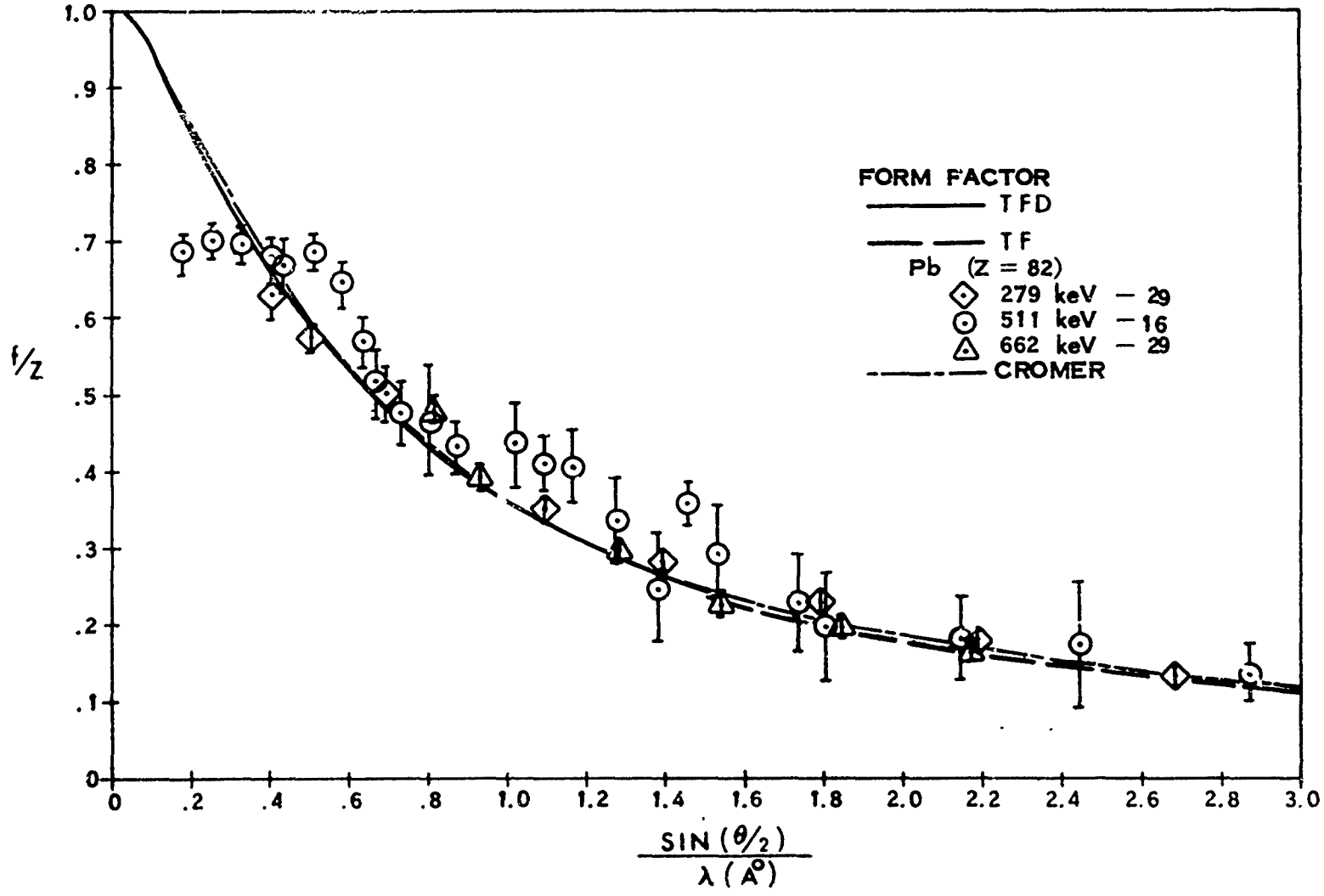
FORM FACTOR
TFD
TF
Pb (Z = 82)
279 keV — 29
511 keV — 16
662 keV — 29
CROMER
f/Z
1.0
.9
.8
.7
.6
.5
.4
.3
.2
.1
0
0
.2
.4
.6
.8
1.0
1.2
1.4
1.6
1.8
2.0
2.2
2.4
2.6
2.8
3.0
SIN (θ/2) / λ (Å)

FIGURE 17

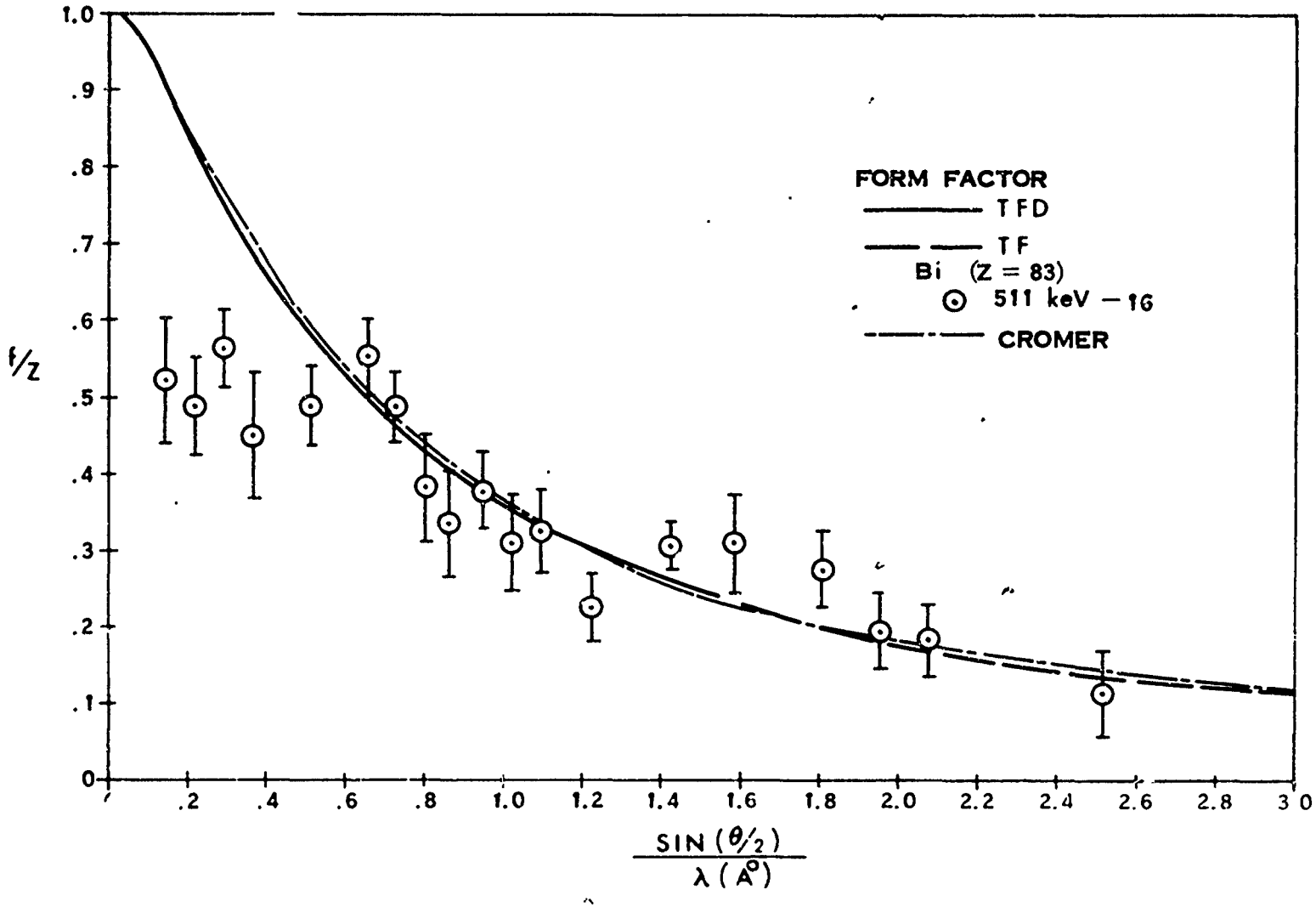
FORM FACTOR
TFD
TF
Bi (Z = 83)
511 keV – 16
CROMER
f/Z
1.0
.9
.8
.7
.6
.5
.4
.3
.2
.1
0
.2
.4
.6
.8
1.0
1.2
1.4
1.6
1.8
2.0
2.2
2.4
2.6
2.8
3.0
SIN (θ/2) / λ (Å)

FIGURE 18

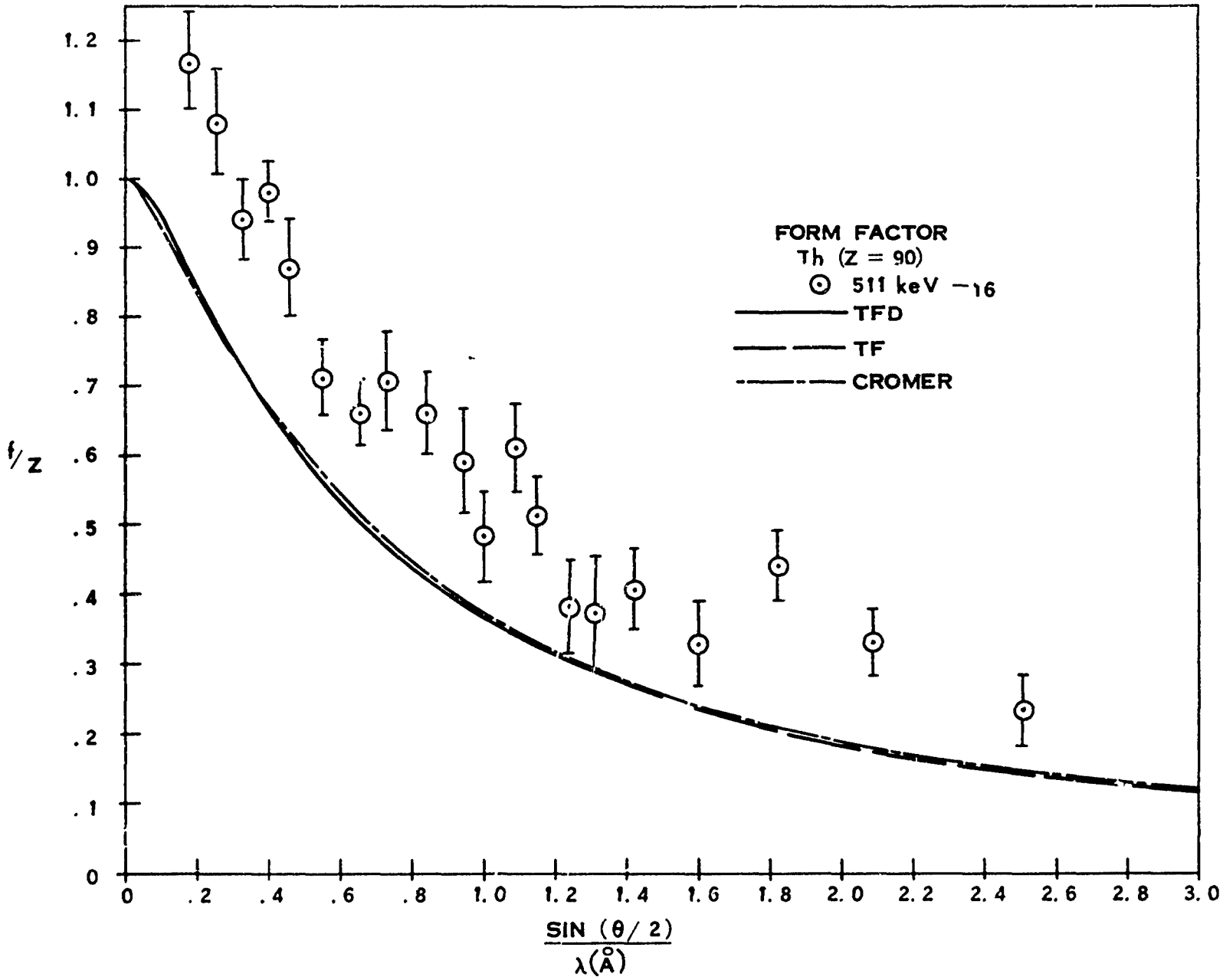
FORM FACTOR
Th (Z = 90)
511 keV −16
TFD
TF
CROMER
f/Z
1.2
1.1
1.0
.9
.8
.7
.6
.5
.4
.3
.2
.1
0
0
.2
.4
.6
.8
1.0
1.2
1.4
1.6
1.8
2.0
2.2
2.4
2.6
2.8
3.0
SIN (θ/2)
λ(Å)

FIGURE 19

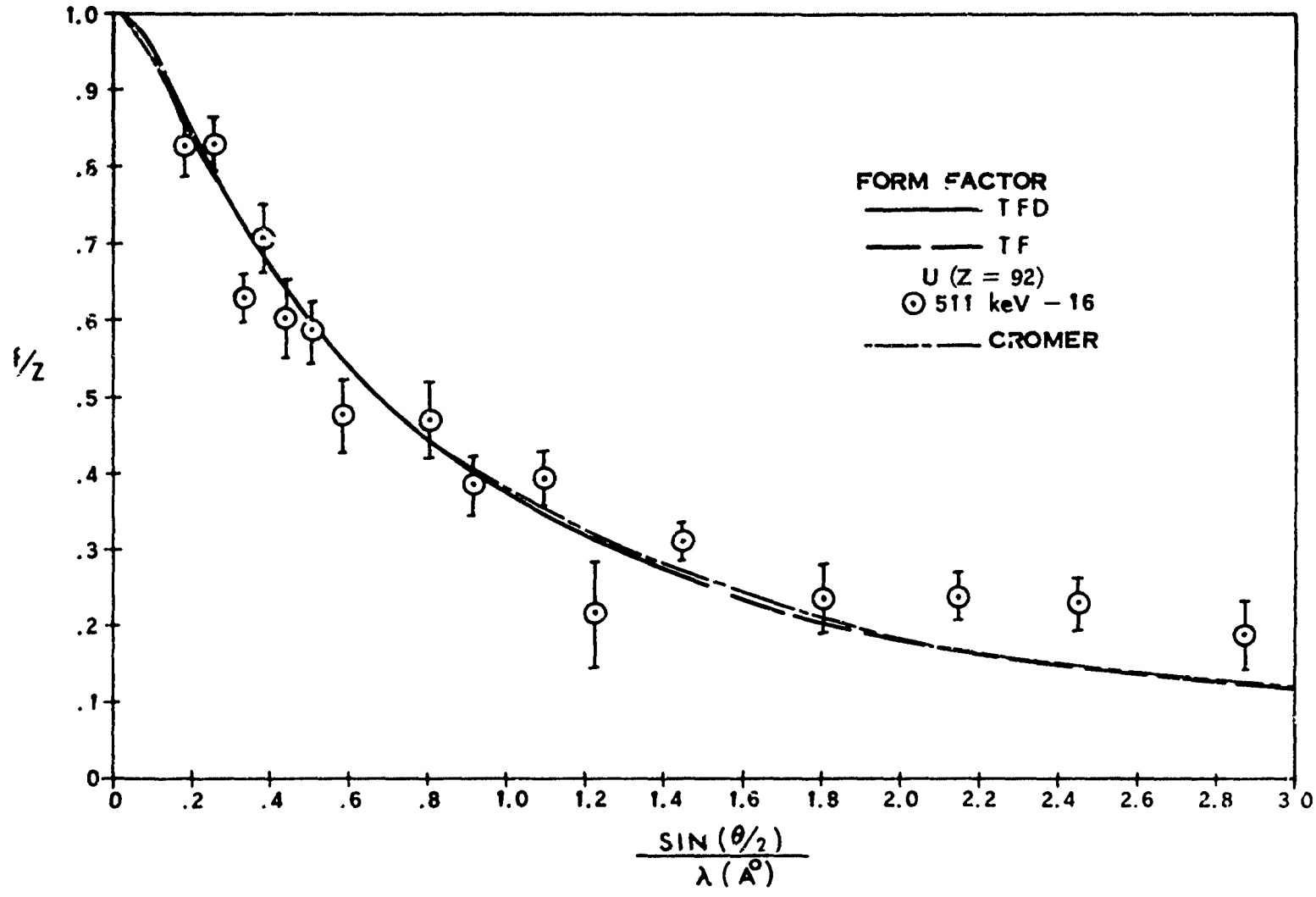
FORM FACTOR
TFD
TF
U (Z = 92)
511 keV – 16
CROMER
f/Z
1.0
.9
.8
.7
.6
.5
.4
.3
.2
.1
0
0
.2
.4
.6
.8
1.0
1.2
1.4
1.6
1.8
2.0
2.2
2.4
2.6
2.8
3.0
SIN (θ/2) / λ (Å)

FIGURE 20

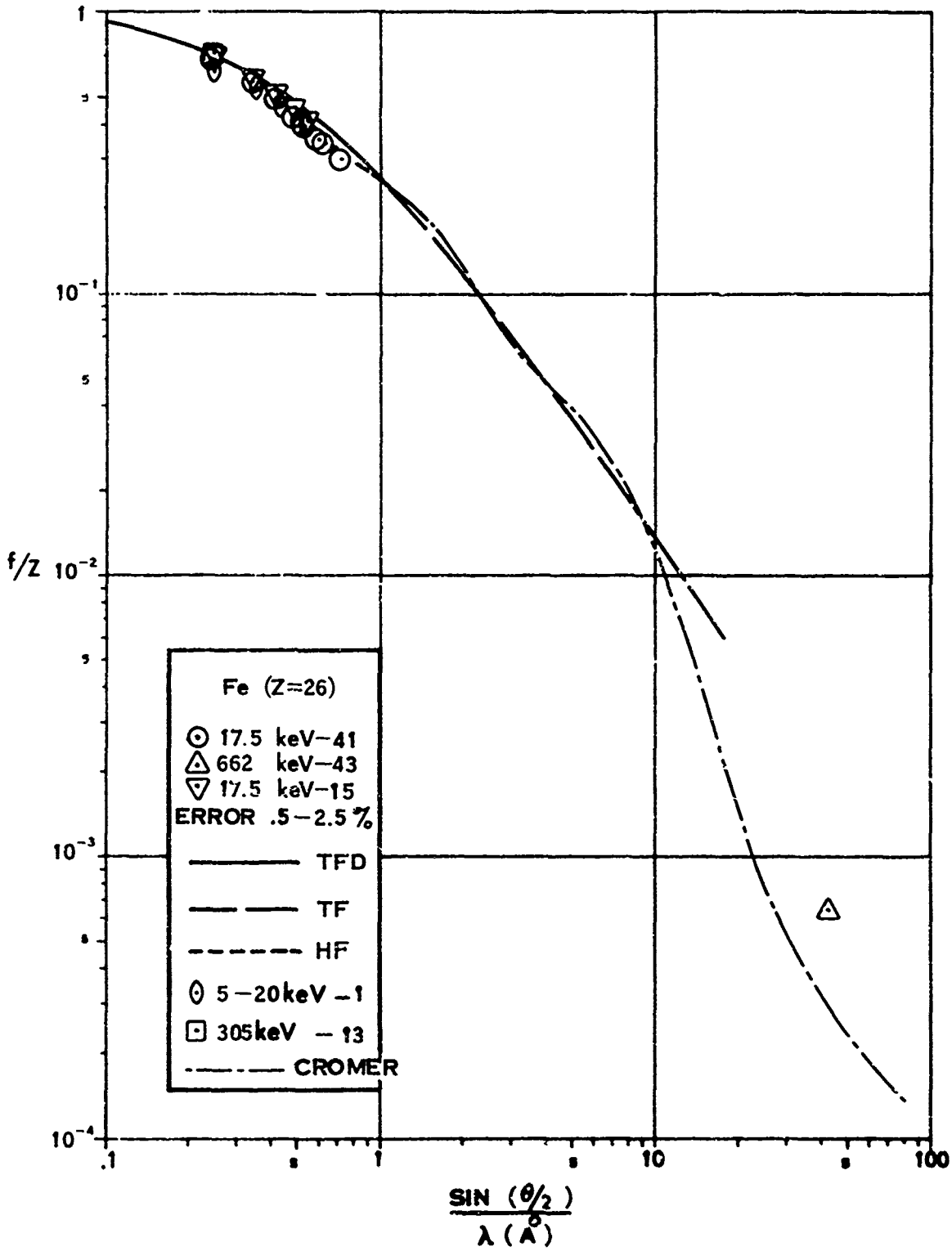
f/Z
1
5
10^{-1}
5
10^{-2}
5
10^{-3}
5
10^{-4}
.1
5
1
5
10
5
100
Fe (Z=26)
17.5 keV–41
662 keV–43
17.5 keV–15
ERROR .5–2.5 %
TFD
TF
HF
5–20keV –1
305keV – 13
CROMER
SIN (θ/2)
λ (Å)

FIGURE 21

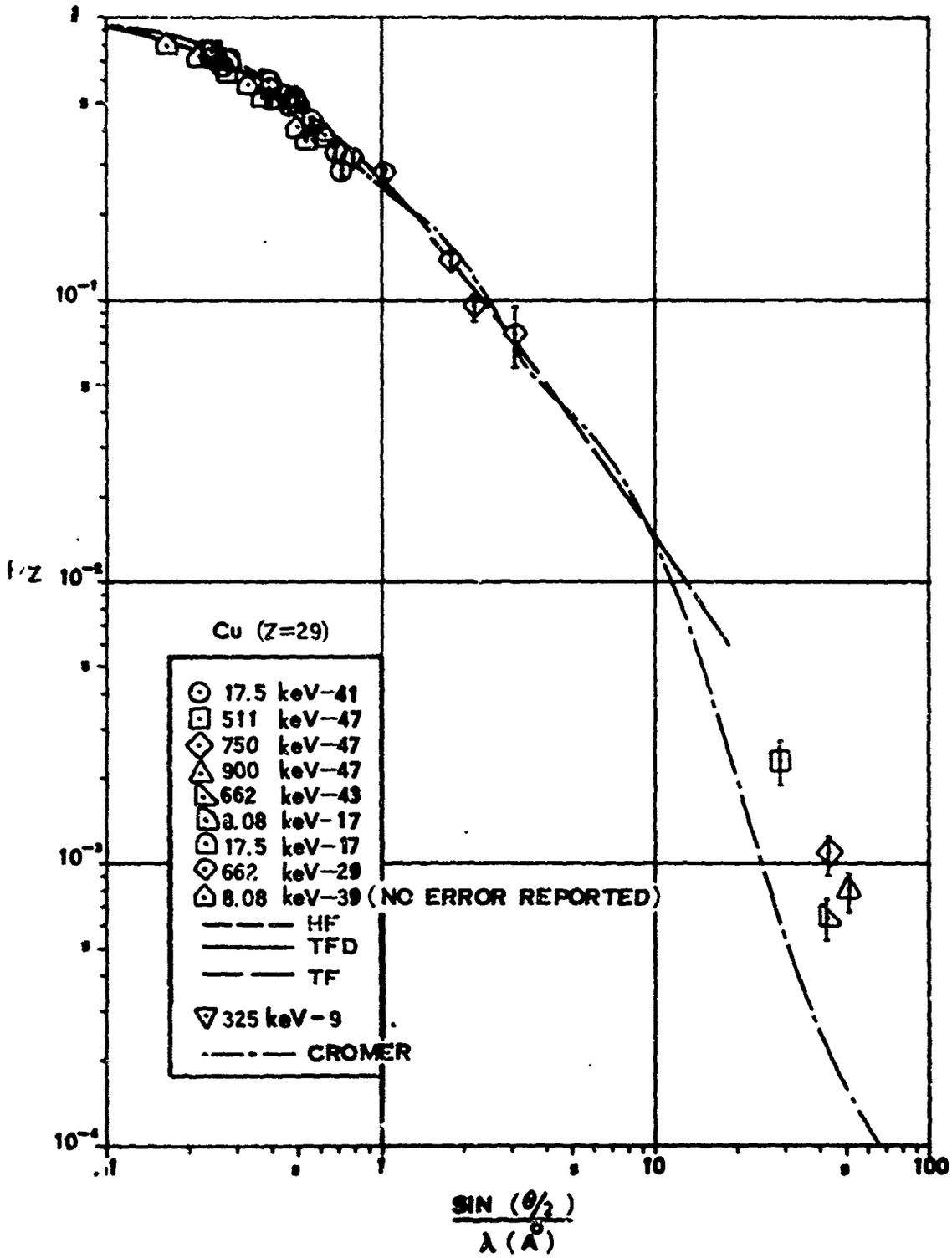
f/Z
Cu (Z=29)
17.5 keV–41
511 keV–47
750 keV–47
900 keV–47
662 keV–43
8.08 keV–17
17.5 keV–17
662 keV–29
8.08 keV–39 (NO ERROR REPORTED)
HF
TFD
TF
325 keV–9
CROMER
SIN (θ/2) / λ (Å)

FIGURE 22

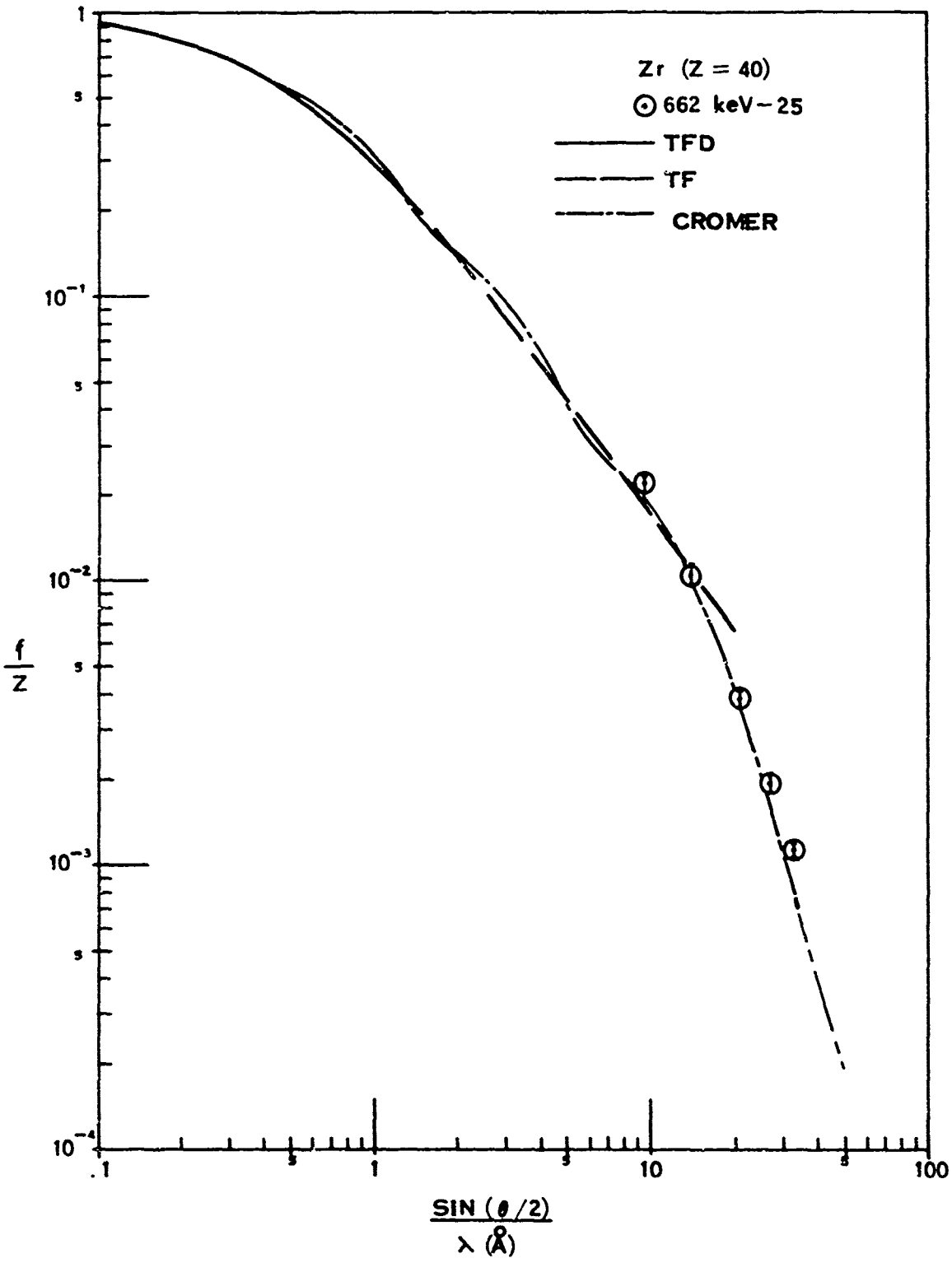
Zr (Z = 40)
662 keV−25
TFD
TF
CROMER
1
5
10^{-1}
5
10^{-2}
5
10^{-3}
5
10^{-4}
f/Z
.1
5
1
5
10
5
100
SIN (θ/2) / λ (Å)

FIGURE 23

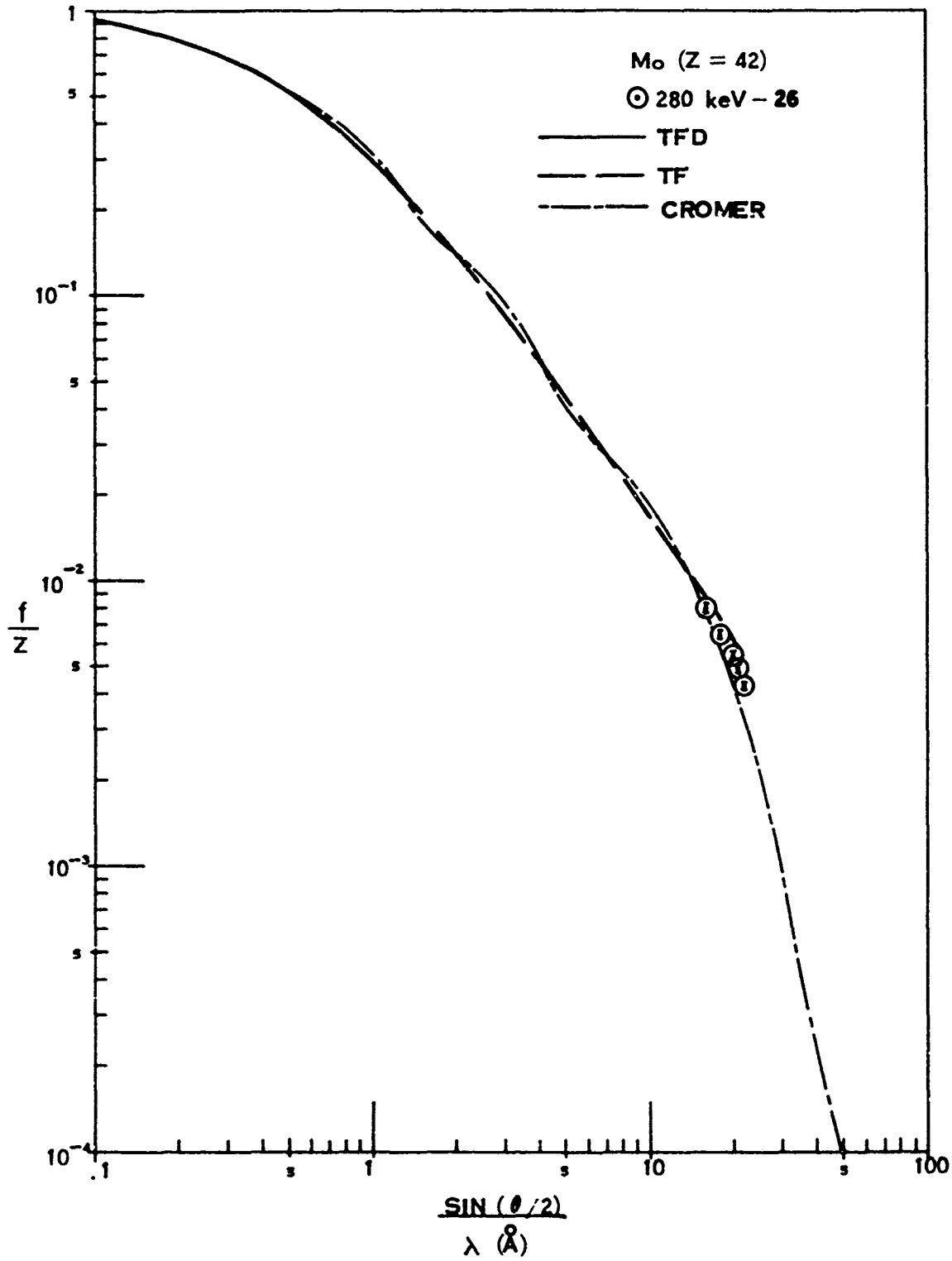
Mo (Z = 42)
280 keV – 26
TFD
TF
CROMER
1
5
10^{-1}
5
10^{-2}
5
10^{-3}
5
10^{-4}
f/Z
.1
5
1
5
10
5
100
SIN (θ/2)/λ (Å)

FIGURE 24

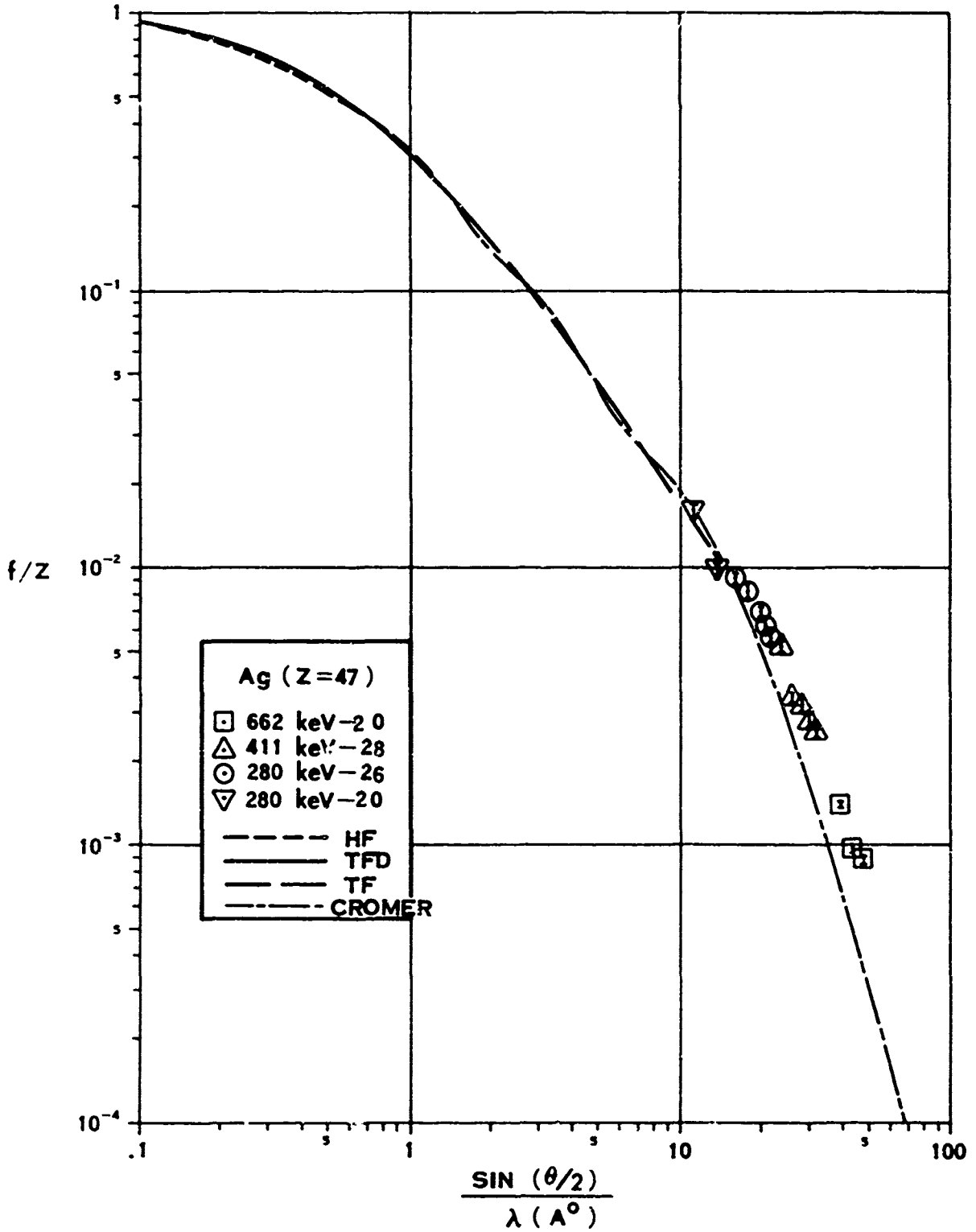
f/Z
1
5
10^{-1}
5
10^{-2}
5
10^{-3}
5
10^{-4}
.1
5
1
5
10
5
100
SIN (θ/2) / λ (A°)
Ag (Z=47)
662 keV−2 0
411 keV−28
280 keV−26
280 keV−20
HF
TFD
TF
CROMER

FIGURE 25

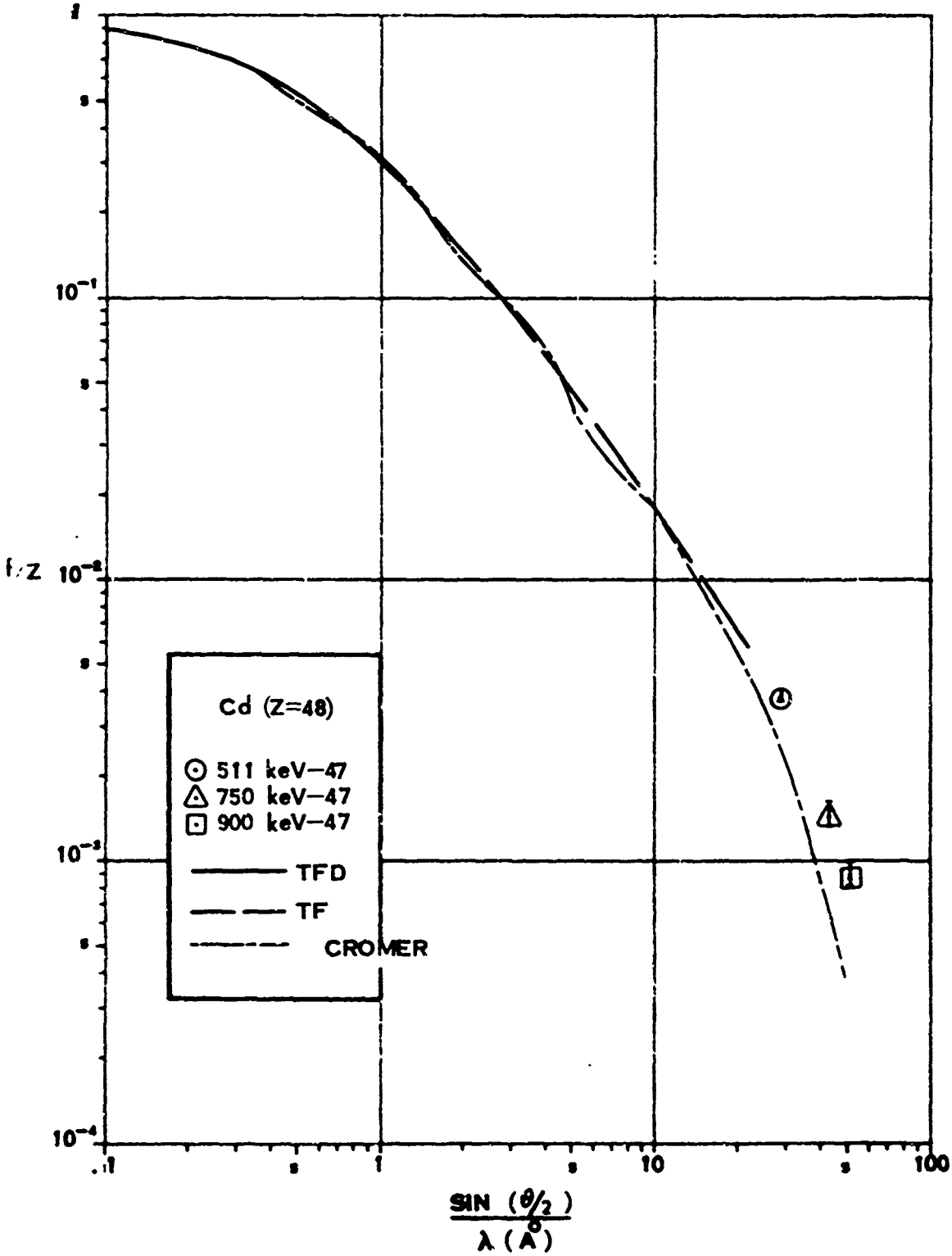
f/Z
1
5
10^{-1}
5
10^{-2}
5
10^{-3}
5
10^{-4}
.1
5
1
5
10
5
100
Cd (Z=48)
511 keV—47
750 keV—47
900 keV—47
TFD
TF
CROMER
SIN (θ/2)
λ (Å)

FIGURE 26

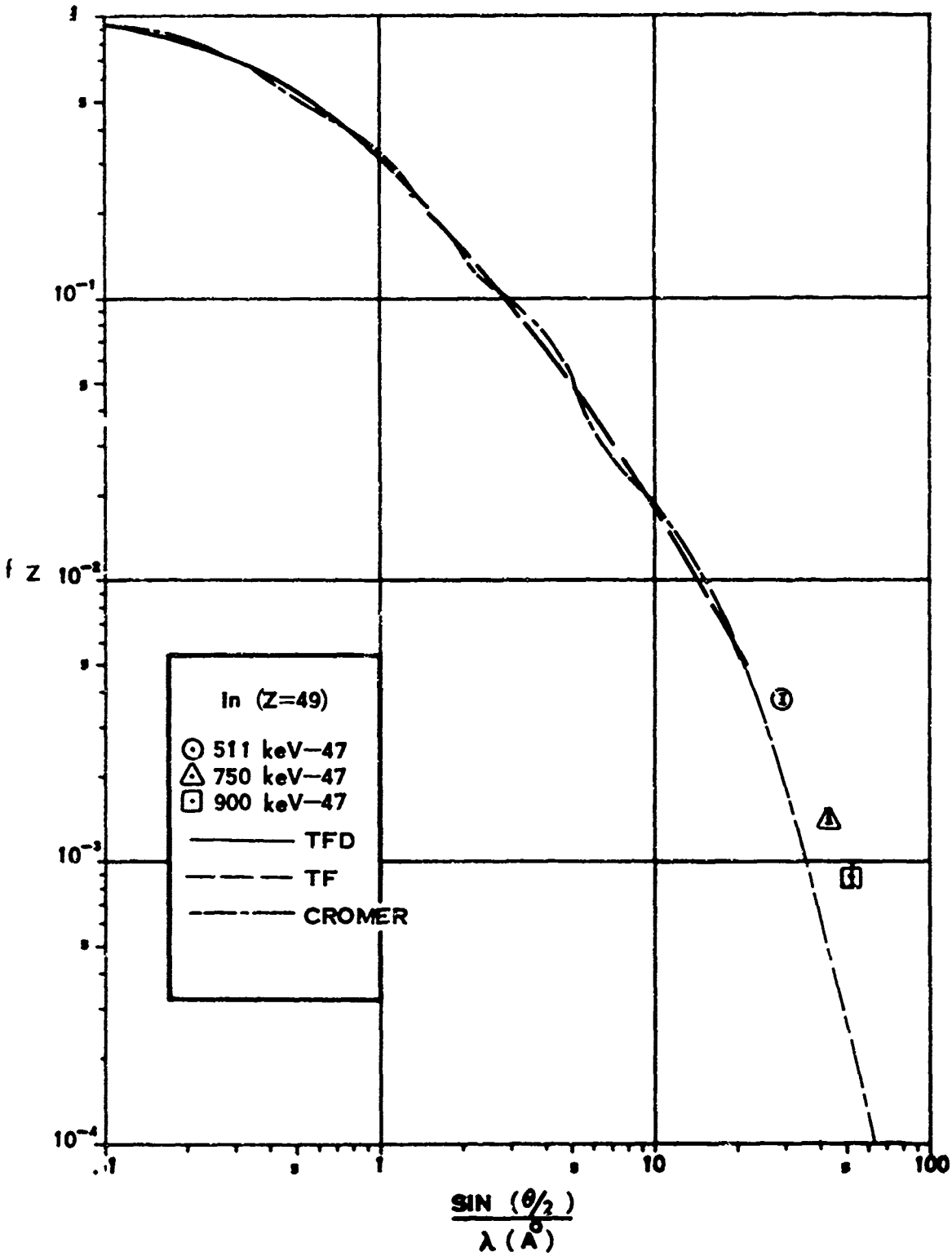
f Z
1
10^{-1}
10^{-2}
10^{-3}
10^{-4}
.1
1
10
100
In (Z=49)
511 keV—47
750 keV—47
900 keV—47
TFD
TF
CROMER
SIN (θ/2)
λ (Å)

FIGURE 27

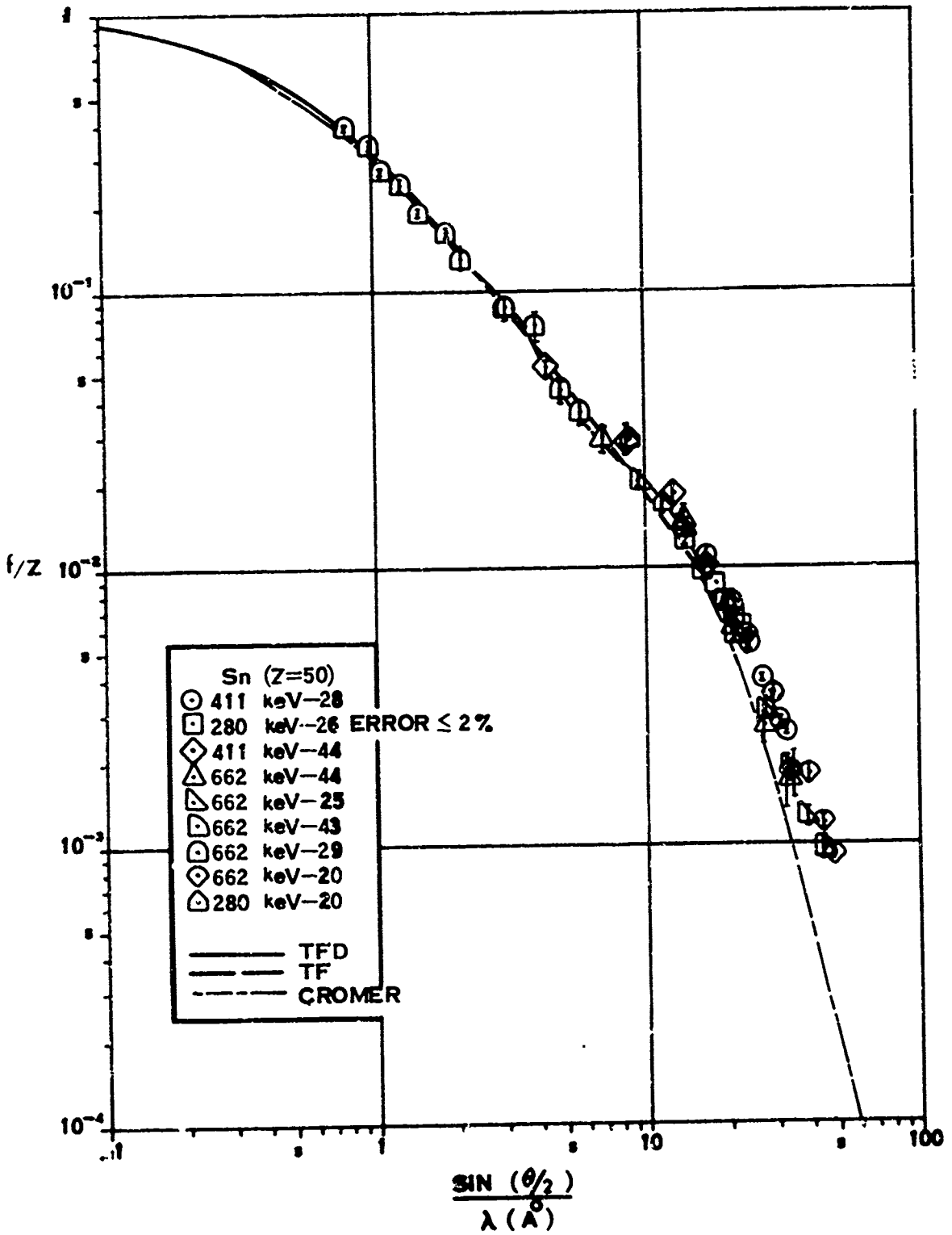
f/Z
Sn (Z=50)
411 keV—28
280 keV—26 ERROR ≤ 2%
411 keV—44
662 keV—44
662 keV—25
662 keV—43
662 keV—29
662 keV—20
280 keV—20
TFD
TF
CROMER
SIN (θ/2)
λ (Å)

FIGURE 28

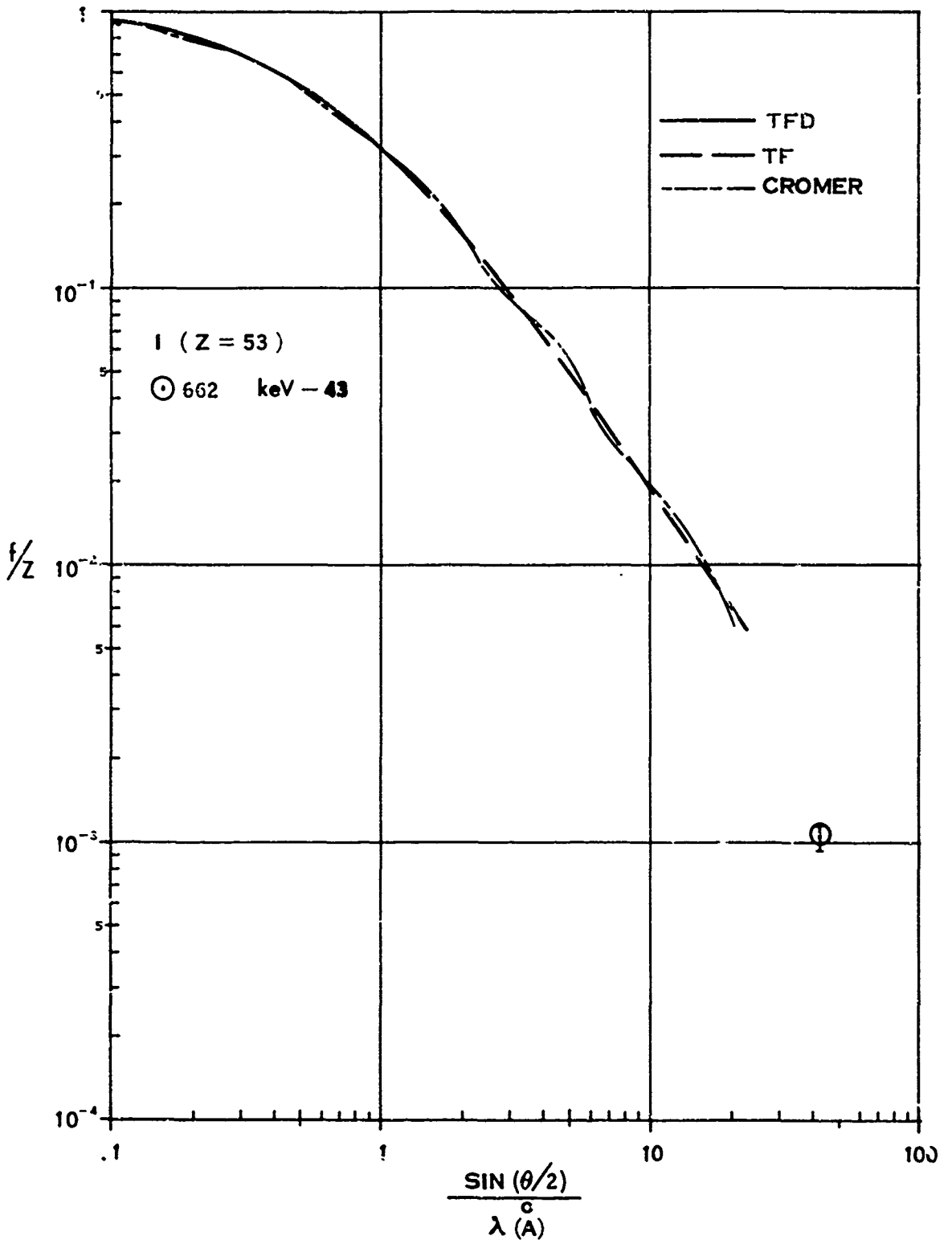
TFD
TF
CROMER
I (Z = 53)
662 keV — 43
f/Z
10^{-1}
10^{-2}
10^{-3}
10^{-4}
.1
1
10
100
SIN (θ/2) / λ (Å)

FIGURE 29

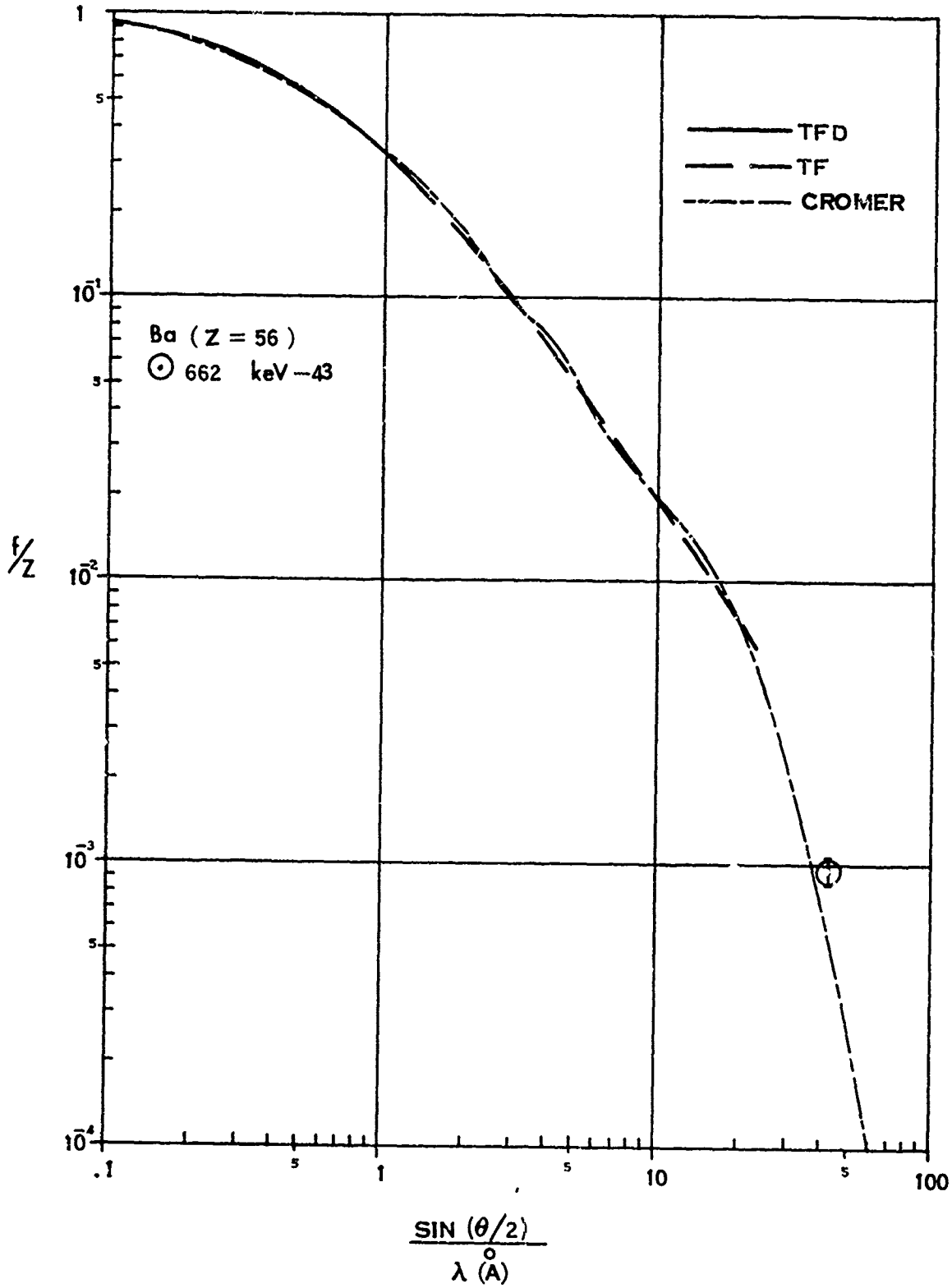
TFD
TF
CROMER
Ba (Z = 56)
662 keV —43
f/Z
1
5
10^{-1}
5
10^{-2}
5
10^{-3}
5
10^{-4}
.1
5
1
5
10
5
100
SIN (θ/2)
λ (Å)

FIGURE 30

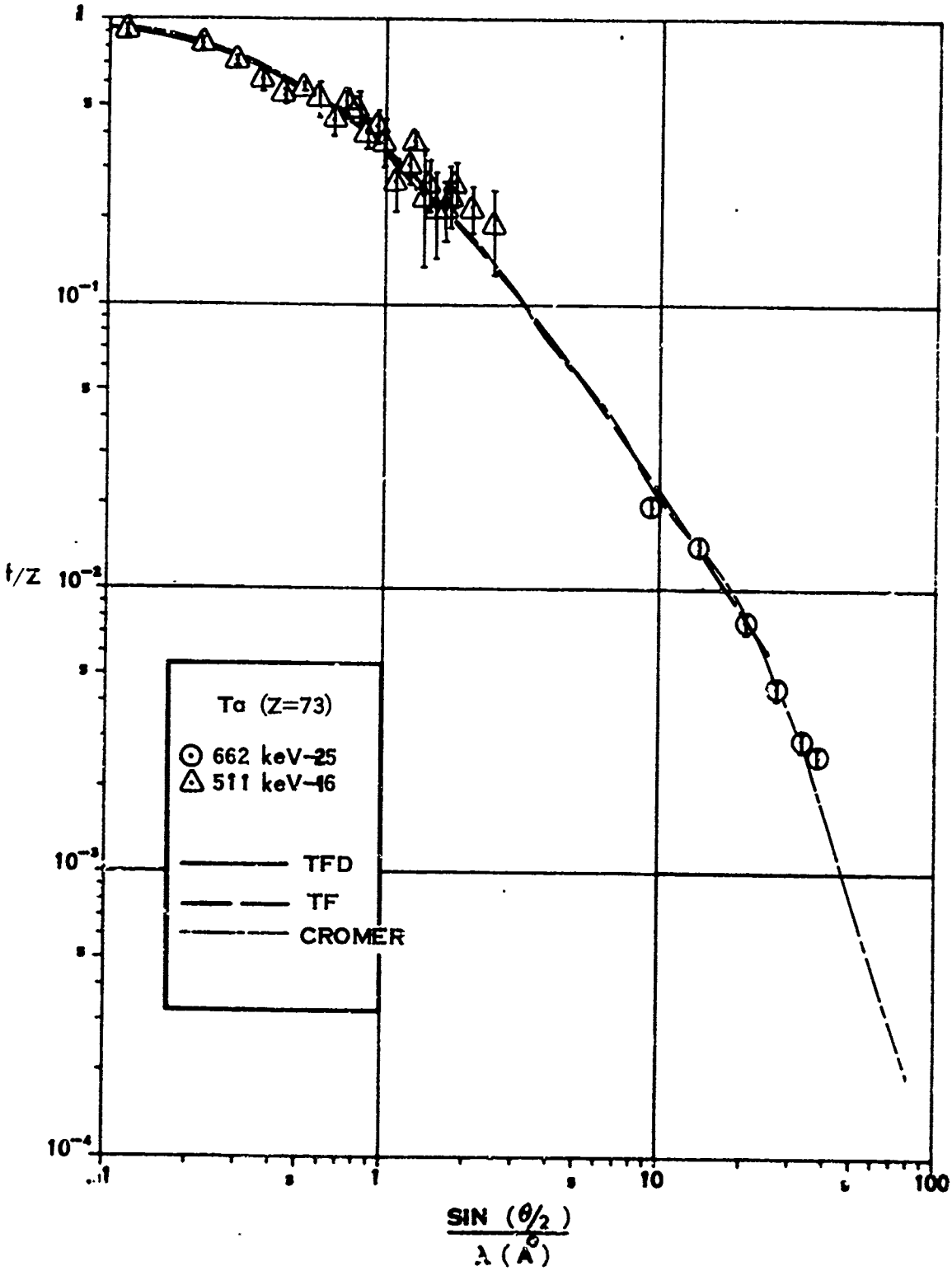

FIGURE 31

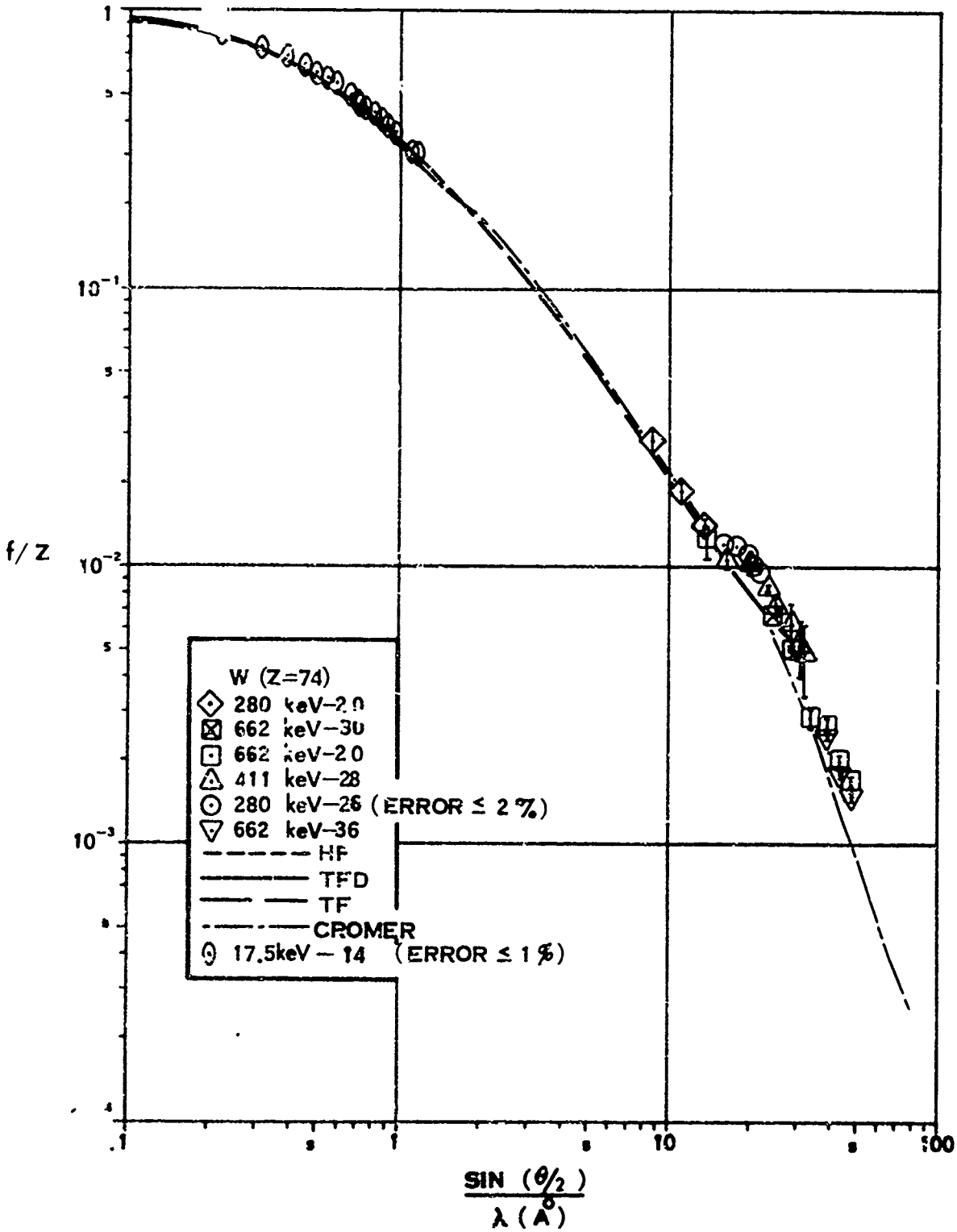
f/Z
W (Z=74)
280 keV–20
662 keV–30
662 keV–20
411 keV–28
280 keV–26 (ERROR ≤ 2 %)
662 keV–36
HF
TFD
TF
CROMER
17.5keV – 14 (ERROR ≤ 1 %)
SIN (θ/2)
λ (Å)

FIGURE 32

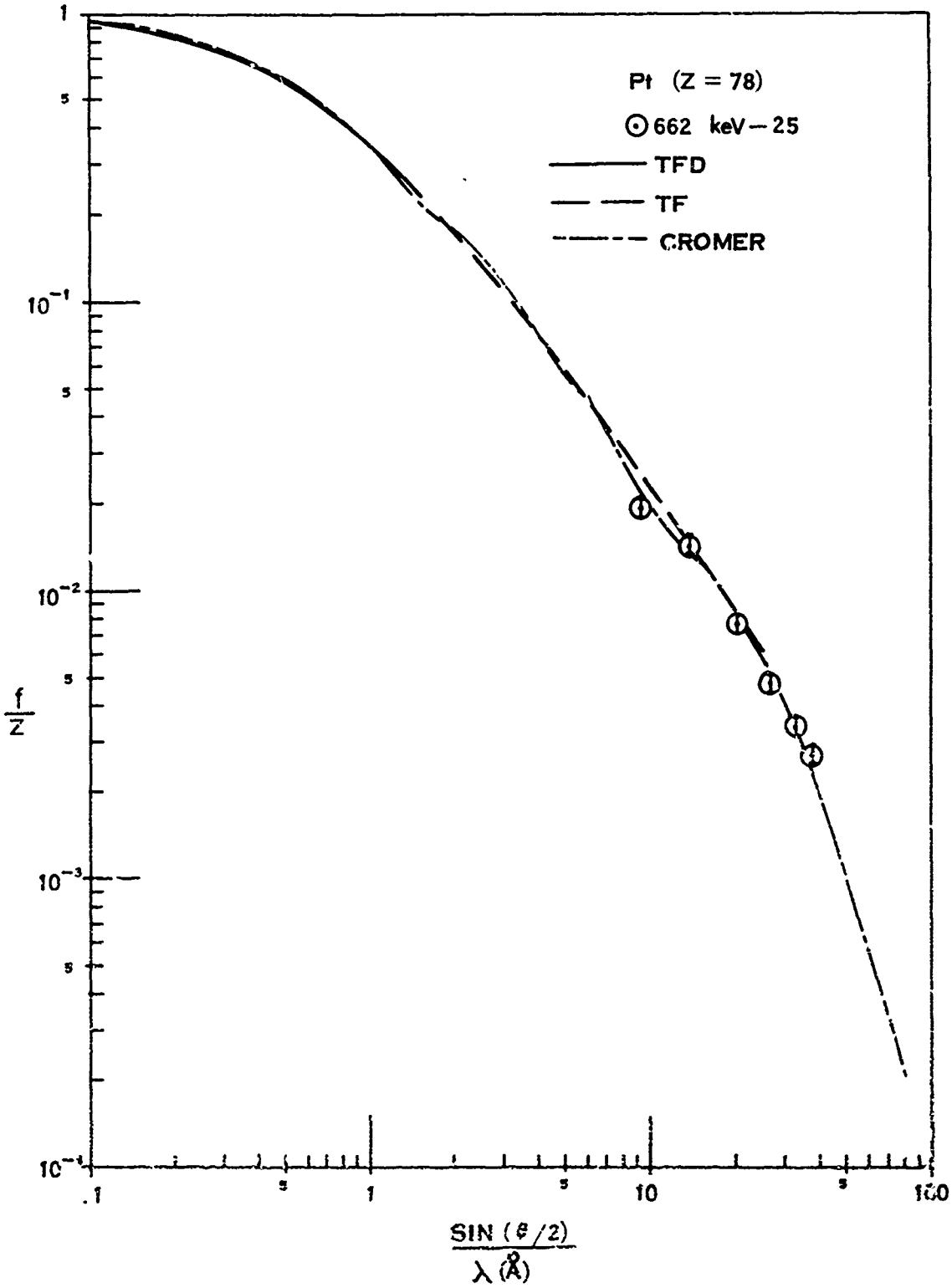
Pt (Z = 78)
662 keV — 25
TFD
TF
CROMER
1
5
10^{-1}
5
10^{-2}
5
10^{-3}
5
10^{-4}
.1
5
1
5
10
5
100
$\frac{f}{Z}$
$\frac{\sin(\theta/2)}{\lambda(\text{Å})}$

FIGURE 33

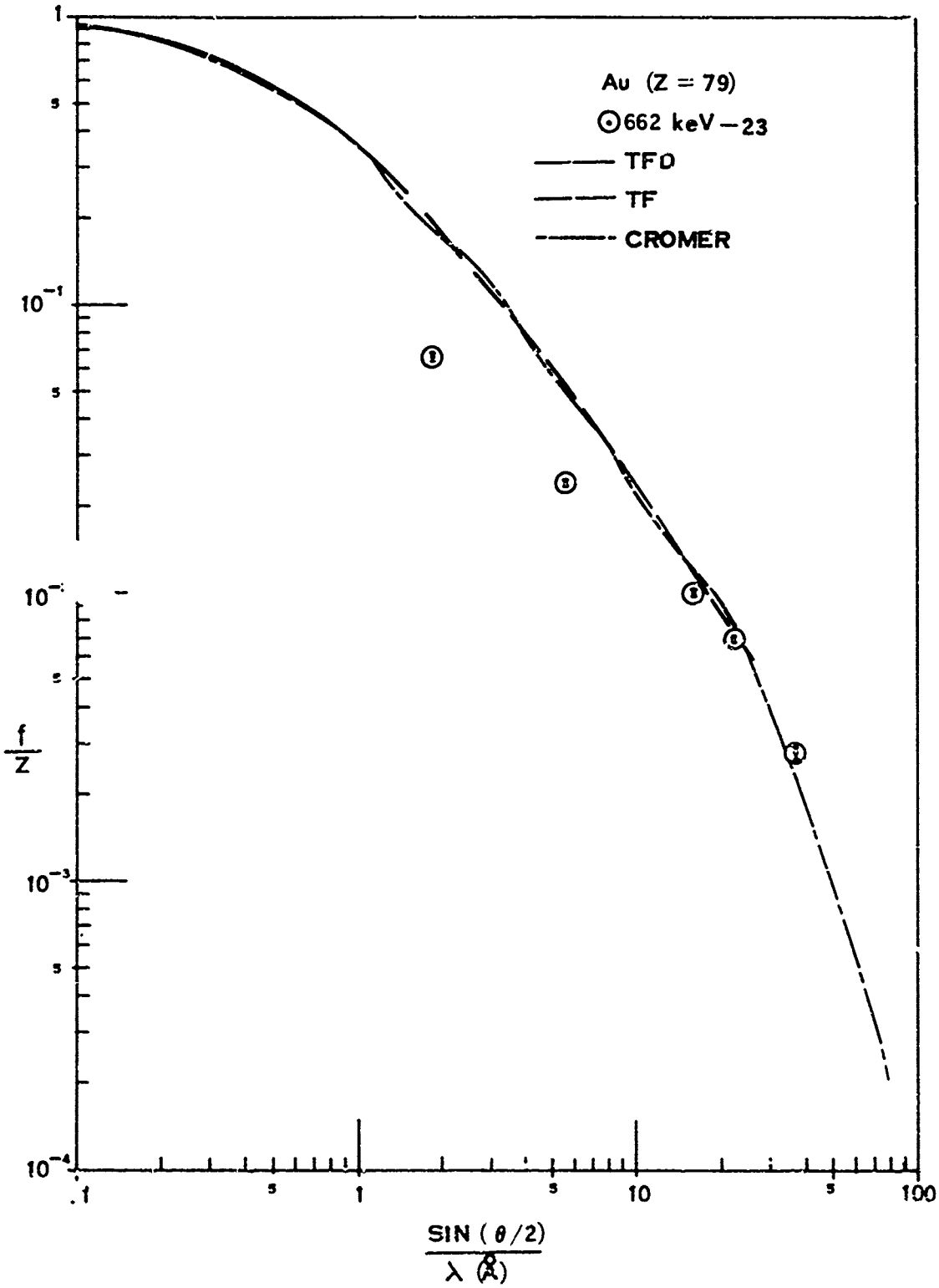
Au (Z = 79)
662 keV −23
TFD
TF
CROMER
1
5
10^{-1}
5
10^{-2}
5
10^{-3}
5
10^{-4}
f/Z
.1
5
1
5
10
5
100
SIN (θ/2) / λ (Å)

FIGURE 34

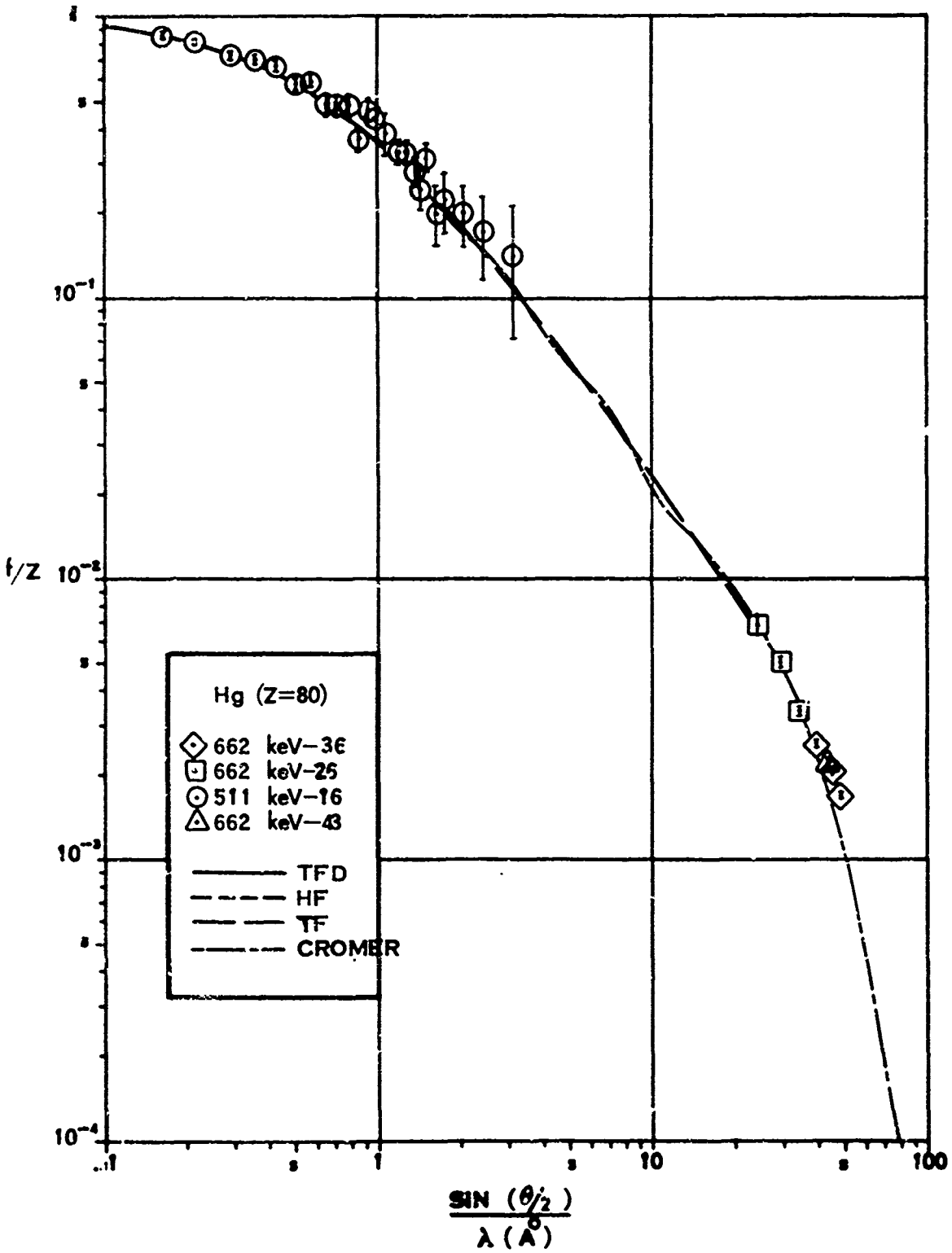
f/Z
Hg (Z=80)
662 keV–36
662 keV–25
511 keV–16
662 keV–43
TFD
HF
TF
CROMER
SIN (θ/2)
λ (Å)

FIGURE 35

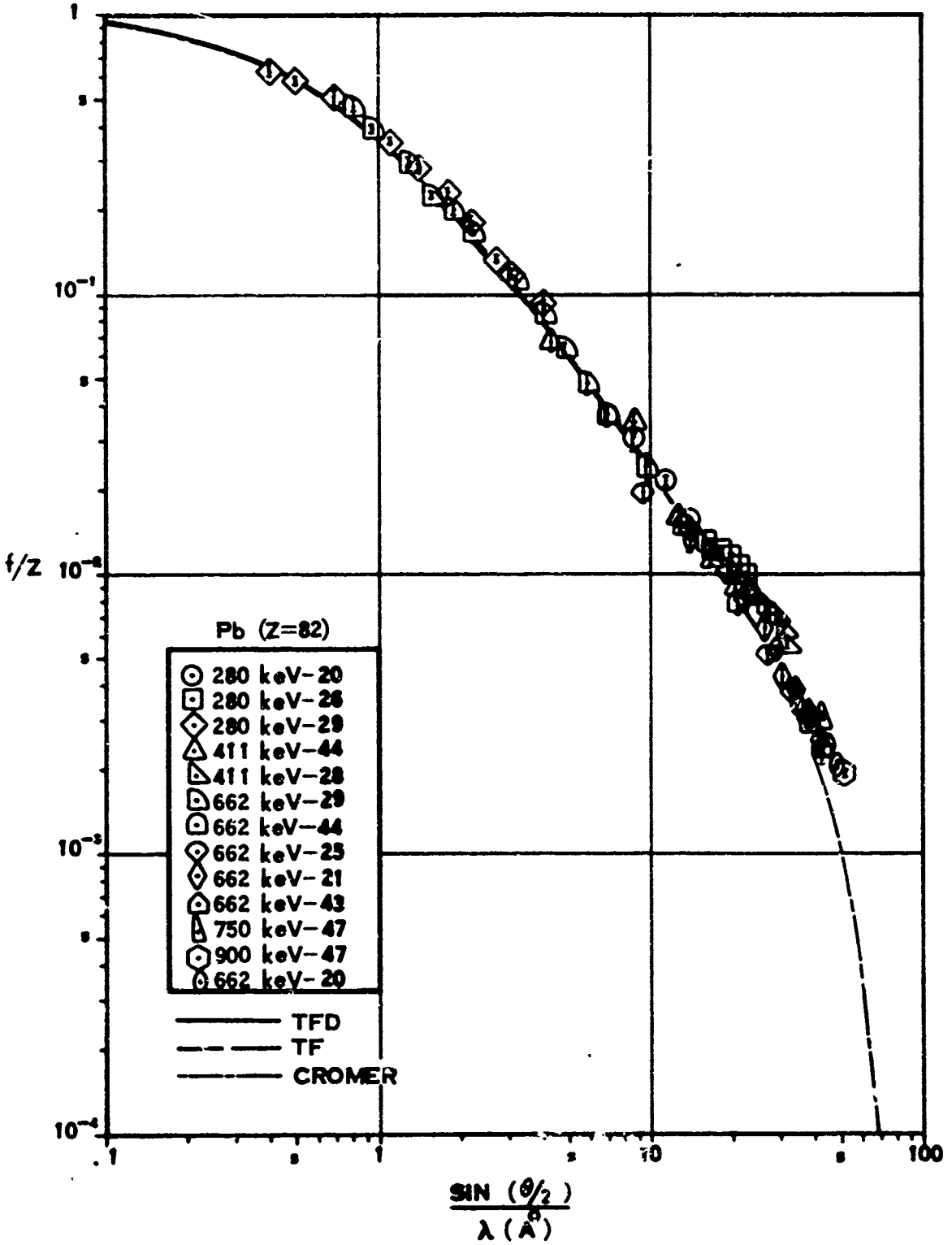
Pb (Z=82)
280 keV-20
280 keV-26
280 keV-29
411 keV-44
411 keV-28
662 keV-29
662 keV-44
662 keV-25
662 keV-21
662 keV-43
750 keV-47
900 keV-47
662 keV-20
TFD
TF
CROMER
f/Z
SIN (θ/2)
λ (Å)

FIGURE 36

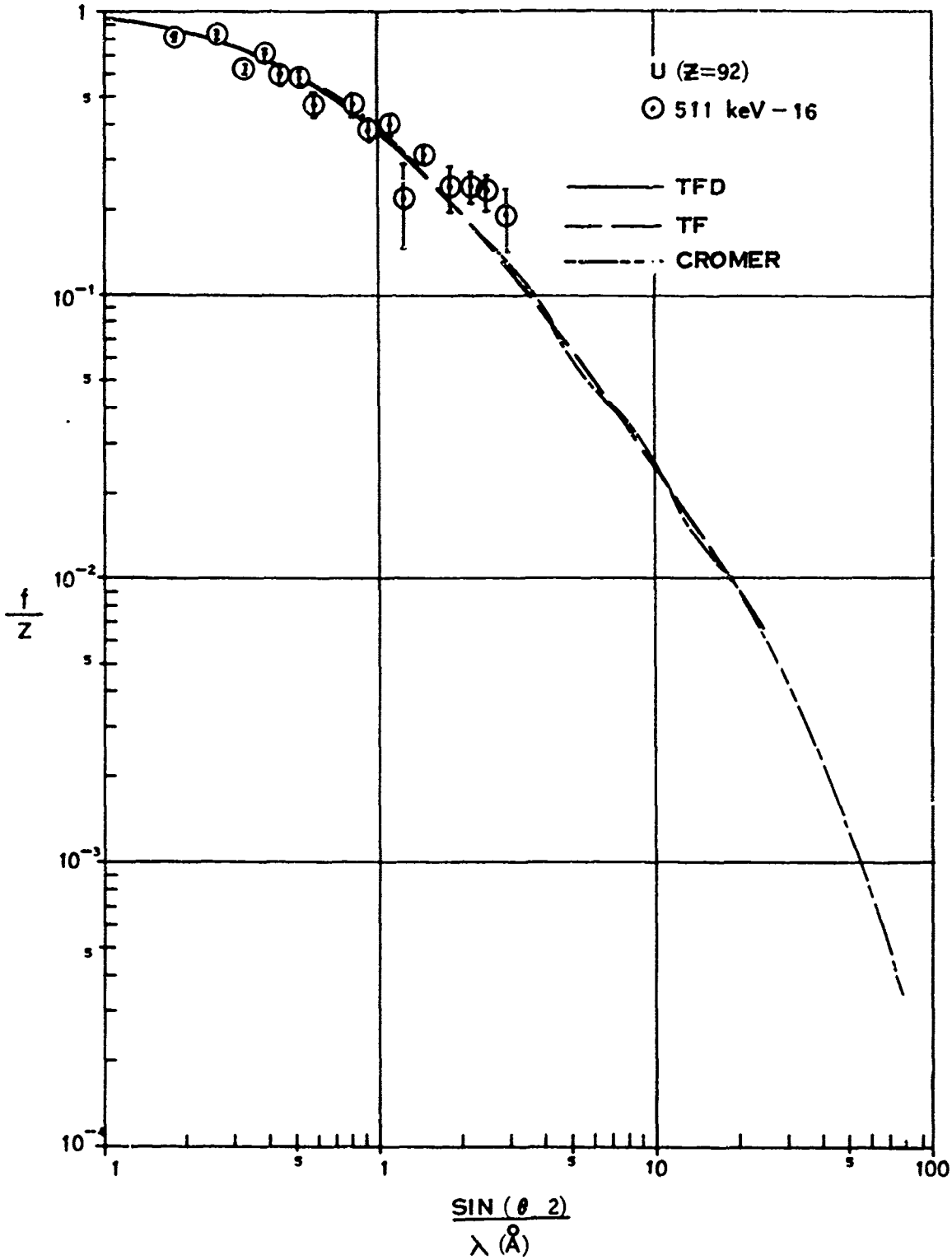

FIGURE 37

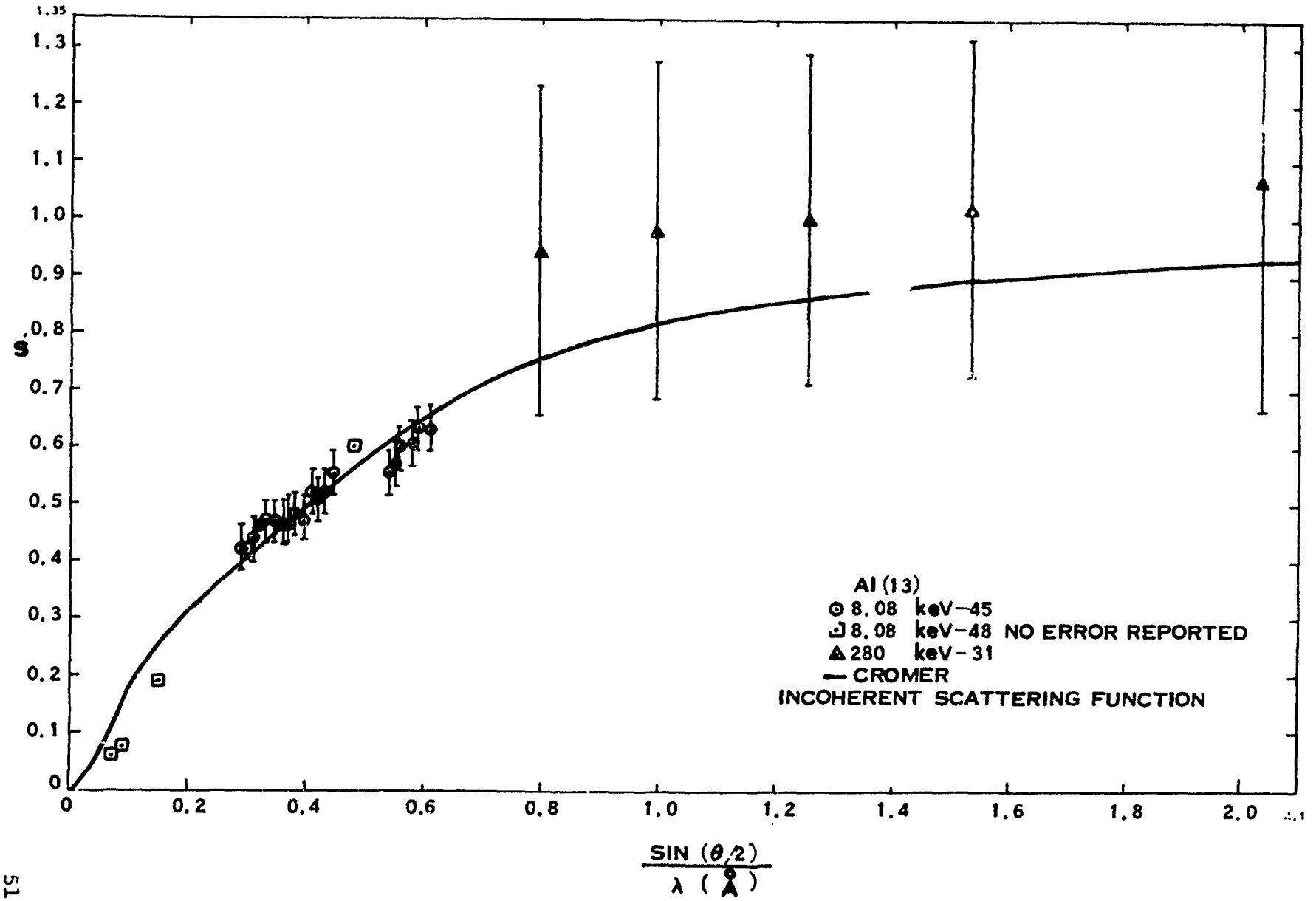
1.35
1.3
1.2
1.1
1.0
0.9
0.8
0.7
0.6
0.5
0.4
0.3
0.2
0.1
0
S
0
0.2
0.4
0.6
0.8
1.0
1.2
1.4
1.6
1.8
2.0
SIN (θ/2)
λ (Å)
Al (13)
8.08 keV–45
8.08 keV–48 NO ERROR REPORTED
280 keV–31
CROMER
INCOHERENT SCATTERING FUNCTION

FIGURE 38

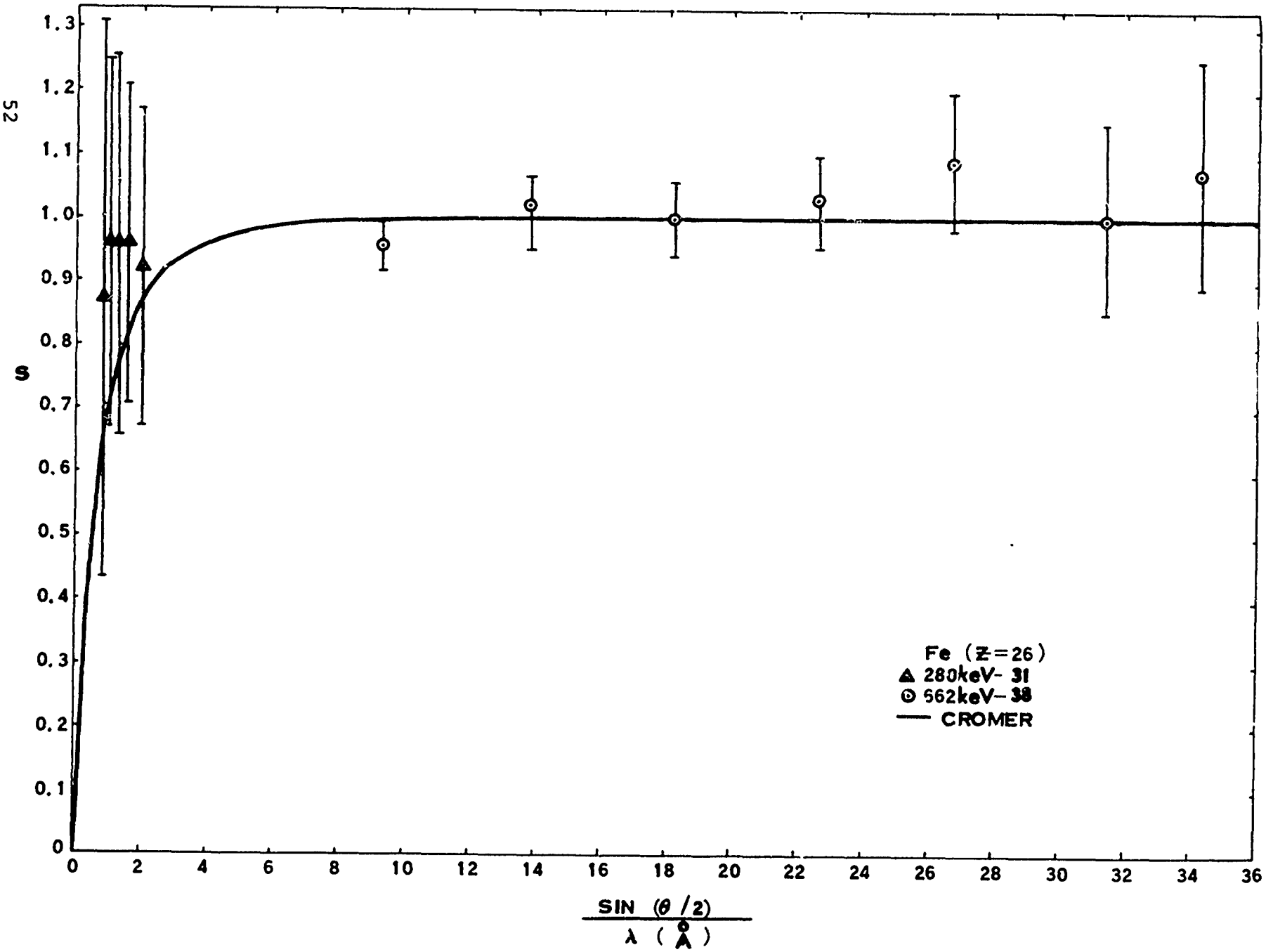
S
1.3
1.2
1.1
1.0
0.9
0.8
0.7
0.6
0.5
0.4
0.3
0.2
0.1
0
0 2 4 6 8 10 12 14 16 18 20 22 24 26 28 30 32 34 36
SIN (θ/2) / λ (Å)
Fe (Z=26)
▲ 280keV- 31
⊙ 562keV- 38
— CROMER

FIGURE 39

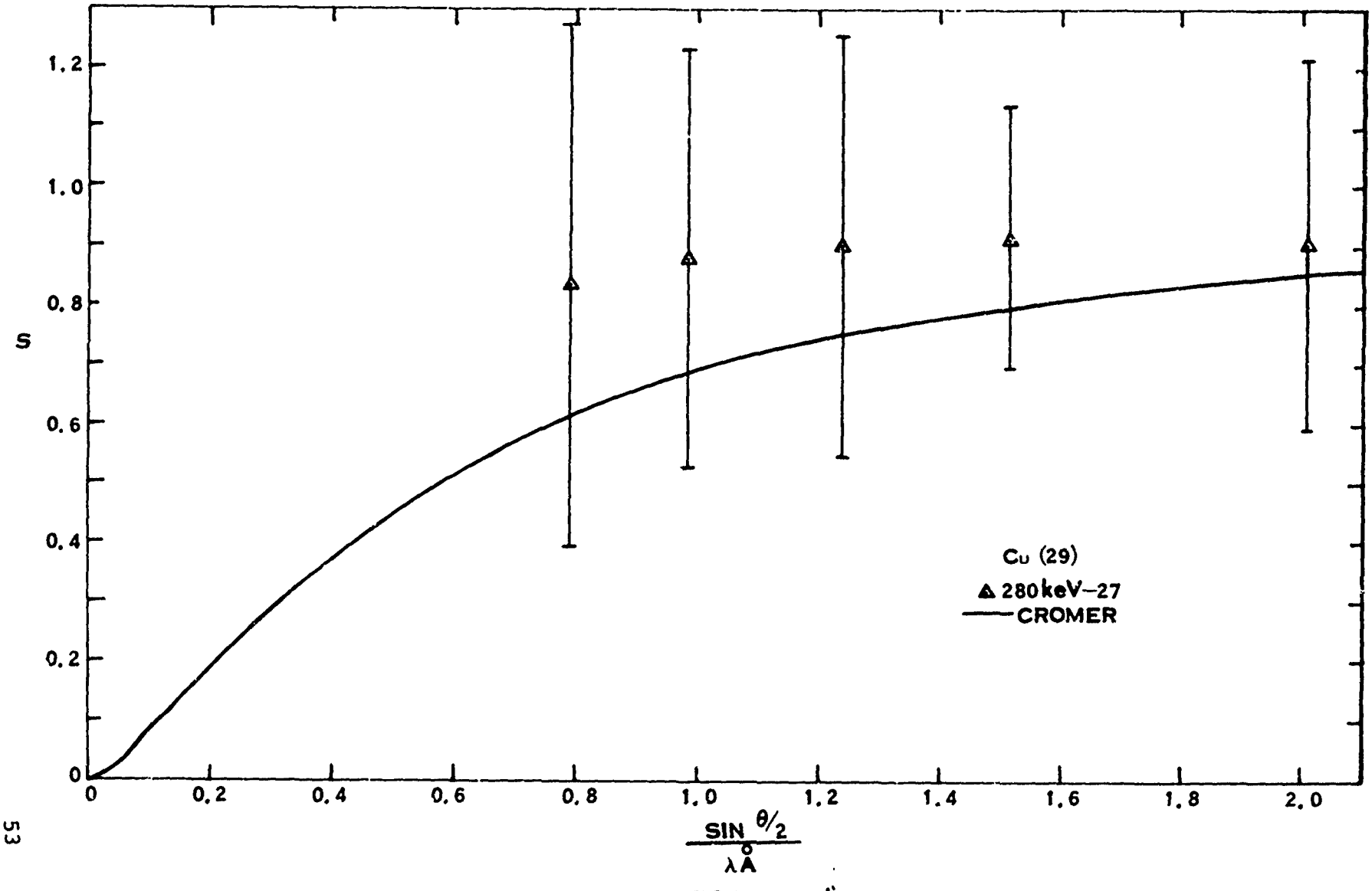
S
1.2
1.0
0.8
0.6
0.4
0.2
0
0
0.2
0.4
0.6
0.8
1.0
1.2
1.4
1.6
1.8
2.0
SIN θ/2
λÅ
Cu (29)
▲ 280keV–27
CROMER

FIGURE 40

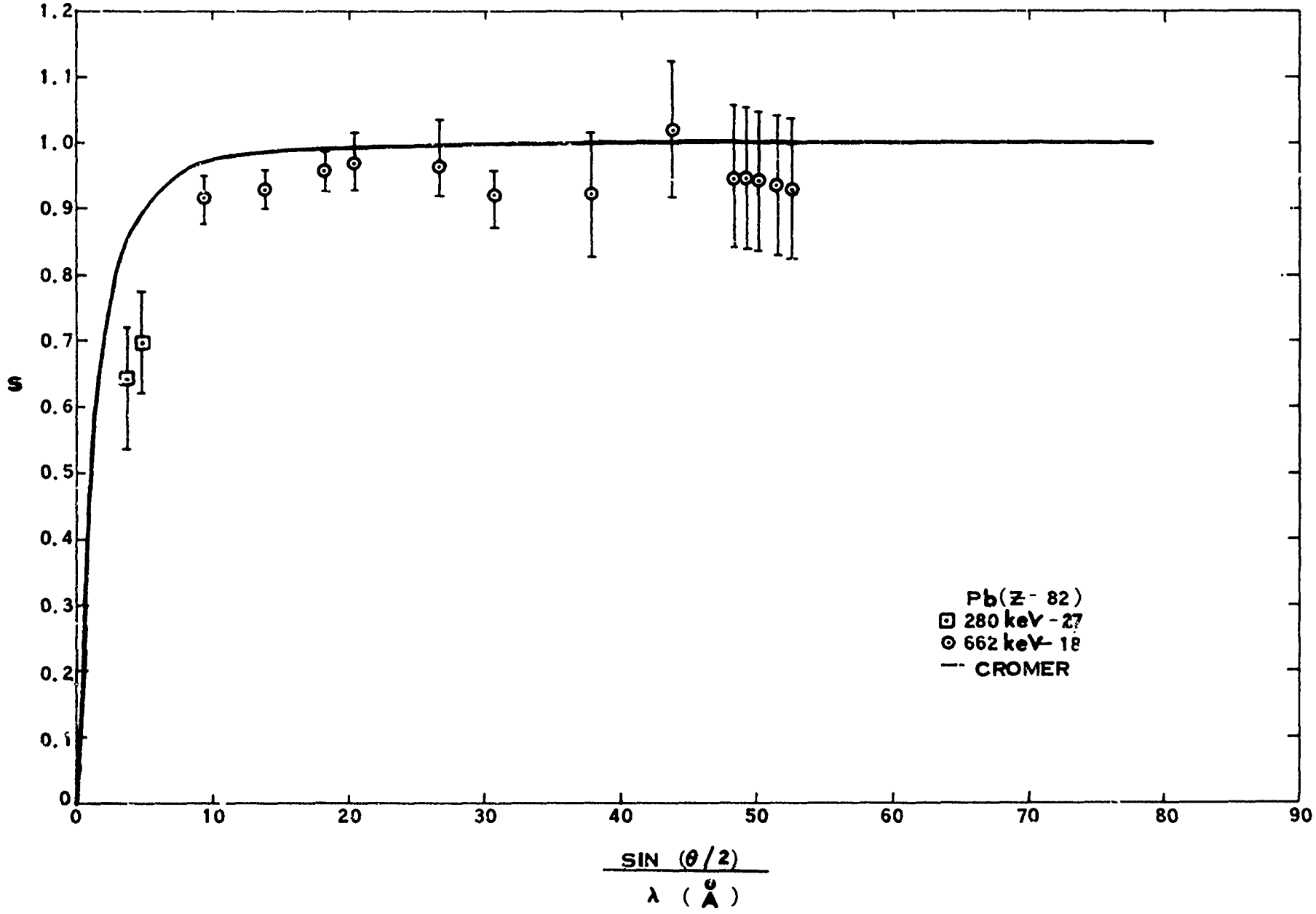
1.2
1.1
1.0
0.9
0.8
0.7
0.6
0.5
0.4
0.3
0.2
0.1
0
S
0
10
20
30
40
50
60
70
80
90
SIN (θ/2)
λ (Å)
Pb(Z- 82)
280 keV - 27
662 keV- 18
CROMER

FIGURE 41

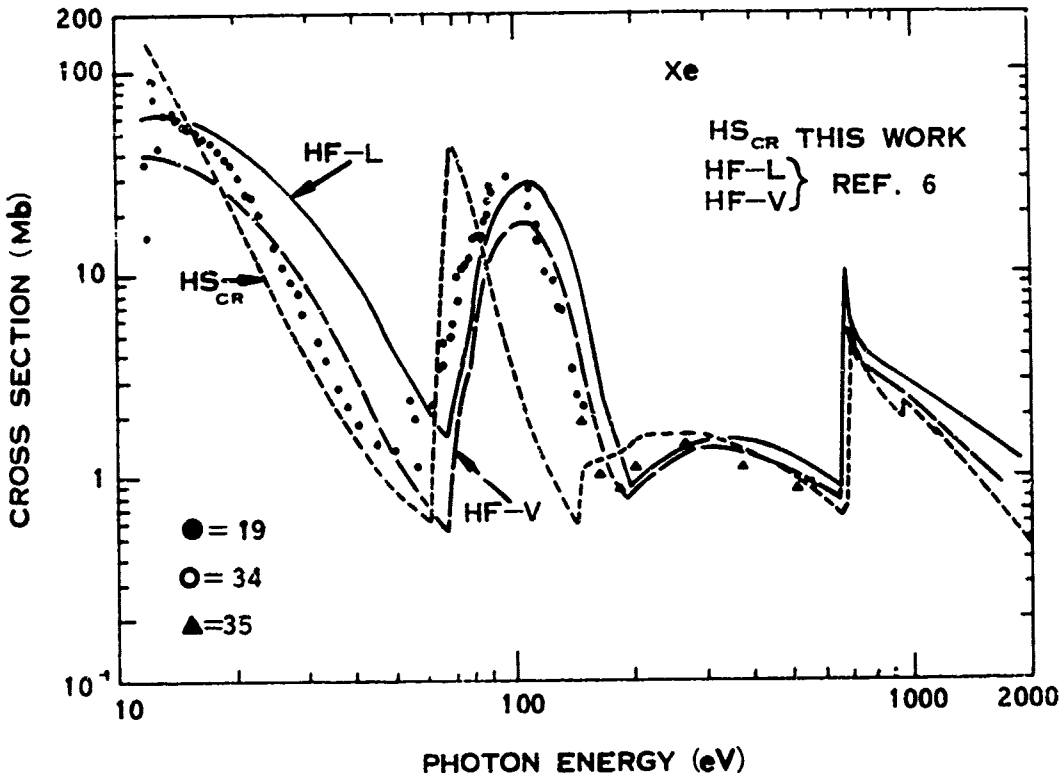
Xe
HS$_{CR}$ THIS WORK
HF–L
HF–V
REF. 6
HF–L
HS$_{CR}$
HF–V
● = 19
O = 34
▲=35
CROSS SECTION (Mb)
PHOTON ENERGY (eV)
200
100
10
1
10^{-1}
10
100
1000
2000

FIGURE 42

APPENDIX A: EXPERIMENTAL DATA SOURCES FOR FIGURES

1970

1. G. G. S. Miller and P. J. Black, Acta Cryst. A 26, 527 (1970).

2. E. Persson, E. Zielinska-Rohozinska, and L. Gerward, Acta Cryst. A 26, 514 (1970).

1969

3. F. O. Halliday, "Differential X-Ray Scattering Cross Section of Beryllium", AFW[illegible]-TR-6[illegible]-133, Stanford Research Institute, Menlo Park, California 94025 (May 1969).

4. P. M. Raccah and V. E. Henrich, Phys. Rev. 184, 607 (1969).

5. M. Jarvinen, M. Merisalo, and O. Inkinen, Phys. Rev. 1[illegible], 1108 (1969).

6. M. Hart and A. D. Milne, Acta Cryst. A 25, 134 (1969).

7. L. D. Jennings, J. Appl. Phys. 40, 5038 (1969).

8. M. Diana, G. Mazzone, and J. J. DeMarco, Phys. Rev. 187, 973 (1969).

9. D. Watanabe, R. Uyeda, and A. Fukuhara, Acta Crist. A 25, 138 (1969).

10. R. M. Middleton and C. P. Gazzara, Phys. Rev. 185, 1230 (1969).

11. K. P. Mamedov, Sov. Phys. - Crystallogr. 14, 113 (1969).

1968

12. B. W. Batterman and J. R. Patel, J. Appl. Phys. 39, 1882 (1968).

13. D. Watanabe, R. Uyeda, and A. Fukuhara, Acta Cryst. A 24, 580 (1968).

14. T. Paakkari and P. Suortti, Phys. Stat. Sol. 28, 539 (1968).

1967

15. T. Paakkari and P. Suortti, Acta Cryst. 22, 755 (1967).

1966

16. U. Hauser and B. Mussgnug, Z. Physik 195, 252 (1966).

17. S. Hosoya and T. Yamagishi, J. Phys. Soc. Japan 21, 2638 (1966).

18. R. Quivy, Nucl. Phys. 76, 362 (1966).

19. J. A. R. Samson in: D. R. Bates and I. Estermann, ed., Advances in Atomic and Molecular Physics, Vol. II, (Academic Press, Inc., N.Y., 1966) p. 178.

1965

20. S. Anand and B. S. Sood, Nucl. Phys. 73, 368 (1965).

21. E. Dahn, Atomkernenergie 10, 39 (1965).

22. J. J. De Marco and R. J. Weiss, Phys. Rev. 137, 1869 (1965).

23. M. A. DiLazzaro and G. Missoni, Ann. Ist. Super. Sanita 1, 1 (1965).

24. H. Hattori et al., J. Phys. Soc. Japan 20, 988 (1965).

25. V. A. Narasimha Murty, V. Lakshminarayana, and S. Jnanananda, Proc. Phys. Soc. 85, 1075 (1965).

1964

26. S. Anand, M. Singh, and B. S. Sood, Current Sci. 33, 333 (1964).

27. S. Anand, M. Singh, and B. S. Sood, Current Sci. 33, 139 (1964).

28. M. Singh, S. Anand, and B. S. Sood, Current Sci. 33, 487 (1964).

29. A. Nath and A. M. Ghose, Nucl. Phys. 57, 547 (1964).

30. M. Singh, S. Anand, and B. S. Sood, Current Sci. 33, 77 (1964)

31. B. S. Sood, M. Singh, and S. Anand, "Incoherent Scattering of 280-keV Gamma Rays", Symposium Proceedings, Feb. 1964. Nucl. Sci. Abstracts 19:17063 (1965).

32. M. J. Cooper, Phil. Mag. 10, 177 (1964).

33. O. Inkinen and P. Suortti, Ann. Acad. Sci. Fennicae A IV, No. 147 (1964).

34. D. L. Ederer, Phys. Rev. Letters 13, 760 (1964).

35. A. P. Lukirskii, I. A. Brytov, and T. M. Zimkina, Opt. Spectrosk (USSR) 17, 438 (1964) English translation in: Opt. Spectrosc. 17, 234 (1964).

1963

36. S. Anand, M. Singh, and B. S. Sood, Current Sci. 32, 401 (1963).

37. D. R. Chipman and L. D. Jennings, Phys. Rev. 132, 728 (1963).

38. M. Singh, S. Anand and B. S. Sood, Indian J. Pure Appl. Phys. 1, 305 (1963).

1962

39. C. J. Sparks and B. S. Borie in: W. M. Mueller and M. Fay, ed., Advances in X-Ray Analysis, Vol. VI (Plenum Press, New York, 1963).

40. M. J. Cooper, Phil. Mag. 7, 2059 (1962).

1961

41. B. W. Batterman, D. R. Chipman, and J. J. DeMarco, Phys. Rev. 122, 68 (1961).

1959

42. S. Göttlicher and E. Wölfel, Z. Elektrochem. 63, 891 (1959).

1958

43. N. Cindro and K. Ilakovac, Nucl. Phys. 5, 647 (1958).

1956

44. A. K. Mann, Phys. Rev. 101, 4 (1956).

45. C. B. Walker, Phys. Rev. 103, 558 (1956).

1955

46. H. Bensch, H. Witte and E. Wölfel, Z. Physik. Chem. (Frankfurt) 4, 65 (1955).

47. J. L. Burkhardt, Phys. Rev. 100, 192 (1955).

1954

48. J. Laval, J. Phys. Radium 15, 657 (1954).